

การเปรียบเทียบเครื่องมือวัดปริมาณรังสีสองระบบ เพื่อตรวจสอบการวางแผนการรักษาการฉาย
รังสีร่วมพิภักในปอด โดยใช้ลำรังสีที่ไม่ผ่านตัวกรอง

นางสาวลิตานัน เมฆนิติกุล

จุฬาลงกรณ์มหาวิทยาลัย
CHULALONGKORN UNIVERSITY

บทคัดย่อและแฟ้มข้อมูลฉบับเต็มของวิทยานิพนธ์ตั้งแต่ปีการศึกษา 2554 ที่ให้บริการในคลังปัญญาจุฬาฯ (CUIR)
เป็นแฟ้มข้อมูลของนิสิตเจ้าของวิทยานิพนธ์ ที่ส่งผ่านทางบัณฑิตวิทยาลัย

The abstract and full text of theses from the academic year 2011 in Chulalongkorn University Intellectual Repository (CUIR)
are the thesis authors' files submitted through the University Graduate School.

วิทยานิพนธ์นี้เป็นส่วนหนึ่งของการศึกษาตามหลักสูตรปริญญาวิทยาศาสตรมหาบัณฑิต

สาขาวิชาฉายาเวชศาสตร์ ภาควิชารังสีวิทยา

คณะแพทยศาสตร์ จุฬาลงกรณ์มหาวิทยาลัย

ปีการศึกษา 2559

ลิขสิทธิ์ของจุฬาลงกรณ์มหาวิทยาลัย

DOSIMETRIC COMPARISON OF PATIENT SPECIFIC QA IN LUNG SBRT
USING UNFLATTENED BEAMS BETWEEN TWO DOSIMETER SYSTEMS

Miss Sitanan Maknitikul



A Thesis Submitted in Partial Fulfillment of the Requirements
for the Degree of Master of Science Program in Medical Imaging
Department of Radiology
Faculty of Medicine
Chulalongkorn University
Academic Year 2016
Copyright of Chulalongkorn University

ลิตานัน เมฆนิตกุล : การเปรียบเทียบเครื่องมือวัดปริมาณรังสีสองระบบ เพื่อตรวจสอบการวางแผนการรักษาการฉายรังสีร่วมพิภักในปอด โดยใช้ลำรังสีที่ไม่ผ่านตัวกรอง (DOSIMETRIC COMPARISON OF PATIENT SPECIFIC QA IN LUNG SBRT USING UNFLATTENED BEAMS BETWEEN TWO DOSIMETER SYSTEMS) อ.ที่ปรึกษาวิทยานิพนธ์หลัก: รศ. ศิวลี สุริยาปี, อ.ที่ปรึกษาวิทยานิพนธ์ร่วม: ดร. ทวีป แสงแห่งธรรม, 66 หน้า.

เครื่องมือที่ใช้สำหรับการประกันคุณภาพของผู้ป่วยเฉพาะบุคคลต้องการความแม่นยำในการวัดปริมาณรังสีเป็นอย่างมากในการฉายรังสีแบบเทคนิคขั้นสูง จุดประสงค์ของการศึกษานี้คือ เพื่อประเมินความแตกต่างของเครื่องมือวัดรังสีสองระบบในการวางแผนการรักษาการฉายรังสีร่วมพิภักในปอด โดยเครื่องมือที่ใช้ในการศึกษาได้แก่ CC13 ion chamber ในหุ่นจำลอง ArcCHECK และ CC13 กับ CC01 ion chamber ในหุ่นจำลอง Lucy เพื่อใช้ในการวัดปริมาณรังสีแบบจุด และ เครื่องมือวัดชนิดไดโอด ในหุ่นจำลอง ArcCHECK กับ ฟิล์มชนิด EBT3 ในหุ่นจำลอง Lucy เพื่อใช้ในการวัดการกระจายปริมาณรังสี โดยใช้เครื่องเร่งอนุภาค Varian TrueBeam ด้วยลำโฟตอน 6MV แบบไม่ผ่านตัวกรอง ระบบการวางแผนการรักษาใช้ Varian Eclipse คำณวนแบบ Acuros XB รุ่น 11.0.31 ในการประเมินสำหรับการตรวจสอบปริมาณรังสีแบบจุด จะใช้เปอร์เซ็นต์ความแตกต่างระหว่างปริมาณรังสีที่วัดได้กับที่คำนวณ และใช้เกณฑ์การผ่านคือ ภายใน $\pm 3\%$ สำหรับระดับที่ควบคุมได้ และ $\pm 5\%$ สำหรับระดับที่จะต้องเฝ้าระวัง ส่วนการตรวจสอบการกระจายปริมาณรังสี จะใช้เปอร์เซ็นต์ Gamma pass ค่าการประเมินความแตกต่างระหว่างปริมาณรังสีที่วัดได้กับที่คำนวณ กำหนดที่ 3% และความแตกต่างของระยะทางที่ 3 mm โดยใช้เกณฑ์การผ่านไม่น้อยกว่า 90% ผลการวัดได้ค่าเฉลี่ยและค่าเบี่ยงเบนมาตรฐานของเปอร์เซ็นต์ความแตกต่างของปริมาณรังสีแบบจุดของ CC13 ion chamber ในหุ่นจำลอง ArcCHECK และ CC13 กับ CC01 ion chamber ในหุ่นจำลอง Lucy เท่ากับ $-1.3 \pm 2.3\%$, $-0.7 \pm 2.3\%$ และ $-1.4 \pm 1.8\%$ ตามลำดับ โดยความสัมพันธ์ของความแตกต่างปริมาณรังสีแบบจุดระหว่าง CC13 ในหุ่นจำลอง ArcCHECK และในหุ่นจำลอง Lucy ไม่แตกต่างกัน เช่นเดียวกับ CC01 กับ CC13 ในหุ่นจำลอง Lucy ไม่มีความแตกต่างกันอย่างมีนัยสำคัญทางสถิติด้วยค่า $p=0.5$ และ $p=0.4$ ตามลำดับ สำหรับการกระจายรังสี ค่าเฉลี่ยและค่าเบี่ยงเบนมาตรฐานของเปอร์เซ็นต์ Gamma pass ของเครื่องมือวัดชนิดไดโอด ในหุ่นจำลอง ArcCHECK กับ ฟิล์มชนิด EBT3 ในหุ่นจำลอง Lucy ได้แก่ $94.9 \pm 1.9\%$ และ $92.6 \pm 5.9\%$ ตามลำดับ โดยความสัมพันธ์ของ gamma pass ระหว่างหัววัดชนิดไดโอดในหุ่นจำลอง ArcCHECK กับ ฟิล์มชนิด EBT3 ในหุ่นจำลอง Lucy ไม่มีความแตกต่างกันอย่างมีนัยสำคัญทางสถิติด้วยค่า $p=0.2$ จากการศึกษาพบว่า ความแตกต่างระหว่างปริมาณรังสีที่วัดได้กับปริมาณรังสีที่ได้จากการคำนวณของแผนการรักษาส่วนใหญ่อยู่ในเกณฑ์ยอมรับได้ โดยความแตกต่างของการวัดปริมาณรังสีแบบจุดคือ $\pm 3\%$ หรือ มีค่าเปอร์เซ็นต์ Gamma pass ไม่น้อยกว่า 90% และพบว่าผลกระทบของขนาดของหัววัดรังสี (ion chamber) และ ชนิดของหุ่นจำลอง ไม่มีความแตกต่างกันอย่างมีนัยสำคัญทางสถิติ อย่างไรก็ตามเครื่องวัดรังสีบางชนิดมีข้อจำกัดในการใช้งาน จึงต้องศึกษาคุณสมบัติเครื่องมือวัดรังสีก่อนการใช้งาน

ภาควิชา รังสีวิทยา

ลายมือชื่อนิติคุณ

สาขาวิชา ฉายาเวชศาสตร์

ลายมือชื่อ อ.ที่ปรึกษาหลัก

ปีการศึกษา 2559

ลายมือชื่อ อ.ที่ปรึกษาร่วม

5874078330 : MAJOR MEDICAL IMAGING

KEYWORDS: STEREOTACTIC BODY RADIATION THERAPY (SBRT) / FLATTENING FILTER FREE (FFF) / PATIENT SPECIFIC QUALITY ASSURANCE / DOSIMETRY SYSTEM

SITANAN MAKNITIKUL: DOSIMETRIC COMPARISON OF PATIENT SPECIFIC QA IN LUNG SBRT USING UNFLATTENED BEAMS BETWEEN TWO DOSIMETER SYSTEMS. ADVISOR: ASSOC. PROF. SIVALEE SURIYAPEE, M.Eng., CO-ADVISOR: TAWEAP SANGHANGTHUM, Ph.D., 66 pp.

In advance technique, the patient specific QA tool needs more accurate dose measurement. The purpose of this study is to determine the dosimetric difference of two dosimeter systems in VMAT lung SBRT. The patient specific QA tools were performed in IBA CC13 in ArcCHECK, IBA CC13 and CC01 in Lucy phantom for point dose and diode array detectors in ArcCHECK and EBT3 film in Lucy phantom for dose distribution in fifteen VMAT lung SBRT plans using unflattened photon beams. All measurements were performed with 6MV FFF photon beam from Varian TrueBeam linear accelerator and the plans were generated using the Varian Eclipse treatment planning system and Acuros XB algorithm (version 11.0.31). For point dose verification, the measured dose and calculated dose were compared by percent point dose difference with criteria $\pm 3\%$ for control limit and $\pm 5\%$ for action limit. For dose distribution verification, the measured dose and calculated dose were compared by percent gamma pass of 3% dose difference and 3 mm distance to agreement with 10% threshold. The criteria were above 90%. For the results of point dose difference, the mean percent point dose difference were $-1.3 \pm 2.3\%$, $-0.7 \pm 2.3\%$ and $-1.4 \pm 1.8\%$ for CC13 in ArcCHECK, CC13 in Lucy phantom and CC01 in Lucy phantom, respectively. The point dose difference between CC13 in ArcCHECK and CC13 in Lucy phantom was not statistical significant difference with p-value = 0.5. And the point dose difference between CC01 and CC13 in Lucy phantom also was not statistical significant difference with p-value = 0.4. For dose distribution verification, the mean percent gamma pass were $94.9 \pm 1.9\%$ and $92.6 \pm 5.9\%$ for diode array detector in ArcCHECK and EBT3 films in Lucy phantom. The gamma pass between diode detector array in ArcCHECK and EBT3 film in Lucy phantom was not statistical significant difference with p-value = 0.2. From the results, the dose differences between calculation and measurement for almost all of the cases were within criteria of $\pm 3\%$ point dose differences or 90% gamma pass for dose distribution differences. The effect on chamber and phantom were not statistical significant difference. However, some dosimeters have limitation for using, the characteristics of dosimeter should be studied before performing the measurement.

Department: Radiology
Field of Study: Medical Imaging
Academic Year: 2016

Student's Signature
Advisor's Signature
Co-Advisor's Signature

ACKNOWLEDGEMENTS

I would like to thank Associate Professor Sivalee Suriyapee, M.Eng, Division of Radiation Oncology, Department of Radiology, Faculty of Medicine, Chulalongkorn University, advisor, to advise, instruct and support for me, Mr. Taweap Sanghantum, Ph.D, co advisor and Mr. Sornjarod Oonsiri, for great suggestion.

I would like to thank Mrs. Puntawa Oonsiri., Mr. Tanawat Tawonwong, Mr. Isra Israngkul Na Ayuthaya, Miss Chotika Jampangern, Mr. Jaruek Kanphet and all of staff in Division of Radiation Oncology, Faculty of Medicine, Chulalongkorn Memorial Hospital for a very kindness suggestion.

I would like to thank Associate Professor Anchali Krisanachinda, Ph.D., Division of Nuclear Medicine, Department of Radiology, Faculty of Medicine, Chulalongkorn University and all lecturers and staff in the Master of Science Program in Medical Imaging, Faculty of Medicine, Chulalongkorn University for their teaching in Medical Imaging.

I would like to thank Dr. Danita Kannarunimit, M.D, Division of Radiation Oncology, Faculty of Medicine, Chulalongkorn Memorial Hospital, who was the chairman of the thesis defense for her suggestion and comments in this research.

I would like to thank Professor Franco Milano, Ph.D, who was the external examiner of the thesis defense for his help, kind suggestion and comments in this research.

Finally, I would like to thank to my family for a very encouragement and financial support.

CONTENTS

	Page
THAI ABSTRACT	iv
ENGLISH ABSTRACT.....	v
ACKNOWLEDGEMENTS.....	vi
CONTENTS.....	vii
LIST OF TABLES	x
LIST OF FIGURES	xii
LIST OF ABBREVIATIONS.....	xv
CHAPTER I.....	1
INTRODUCTION	1
1.1 Background and rationale	1
1.2 Research objectives	2
CHAPTER II.....	3
REVIEW OF RELATED LITERATURES.....	3
2.1 Theories	3
2.1.1 Stereotactic technique.....	3
2.1.1.1 Stereotactic for treating intracranial lesions.....	3
2.1.1.2 Stereotactic for treating extracranial lesions	4
2.1.2 Volumetric modulated arc therapy (VMAT).....	8
2.1.3 Treatment technique for lung cancer.....	9
2.1.3.1 Lung cancer	9
2.1.3.2 Radiotherapy treatment technique for lung cancer.....	10
2.1.4 Flattening filter free.....	12
2.1.5 Patient specific quality assurance	14
2.1.6 Plan evaluation	15
2.1.6.1 The percent point dose difference	15
2.1.6.2 Gamma evaluation method.....	15
2.1.7 Dosimeter	17
2.1.7.1 Ionization chamber	17

	Page
2.1.7.2 Diode array detector (ArcCHECK)	18
2.1.7.3 Radiochromic film [19]	19
2.2 Review of related literatures	21
CHAPTER III	23
RESEARCH METHODOLOGY	23
3.1 Research design	23
3.2 Research design model	23
3.3 Conceptual frame works	24
3.4 Keyword	24
3.5 Research questions.....	25
3.5.1 Primary question.....	25
3.6 Materials	25
3.6.1 Radiation beams	25
3.6.2 Virtual water slab phantom	26
3.6.3 ArcCHECK (3D diode array detector).....	26
3.6.4 Lucy 3D phantom.....	27
3.6.5 The IBA 0.01 and 0.13 cc ionization chamber.....	27
3.6.7 Gafchromic film	28
3.6.8 Film scanner	29
3.6.9 Eclipse Treatment Planning System.....	29
3.6.10 Evaluation software	30
3.7 Method.....	31
3.7.1 Film calibration	31
3.7.2 ArcCHECK calibration	32
3.7.3 Point dose verification.....	32
3.7.4 Dose distribution verification.....	36
3.7.5 Data collection.....	39
3.7.6 Data analysis.....	39
3.7.6.1 Point dose verification.....	39

	Page
3.7.6.2 Dose distribution verification	39
3.7.6.3 Statistical analysis	41
3.8 Outcome measurement	41
3.9 Benefit of the study	41
3.10 Ethical consideration	41
CHAPTER IV	43
RESULTS	43
4.1 Film calibration	43
4.2 Point dose verification	44
4.3 Dose distribution verification	49
CHAPTER V	52
DISCUSSION AND CONCLUSION	52
5.1 Discussion	52
5.1.1 Point dose verification	52
5.1.2 Dose distribution verification	53
5.2 Conclusion	56
5.3 Recommendation	56
REFERENCES	57
APPENDIX	60
VITA	66

LIST OF TABLES

Table 2.1 The comparison of typical characteristics of 3D/IMRT radiotherapy and SBRT[1].	5
Table 2.2 The different characteristics between with and without flattening filter of Varian TrueBeam.	13
Table 4.1 The data of dose, pixel value and optical density of film calibration.	43
Table 4.2 The measured, calculated point dose and point dose difference of fifteen plans using CC13 ion chamber in ArcCHECK.	45
Table 4.3 The measured, calculated point dose and point dose difference of fifteen plans using CC13 ion chamber in Lucy phantom.	46
Table 4.4 The measured, calculated point dose and point dose difference of fifteen plans using CC01 ion chamber in Lucy phantom.	46
Table 4.5 The difference between percent point dose of fifteen plans using CC13 ion chamber in ArcCHECK and Lucy phantom.	47
Table 4.6 The difference between percent point dose of fifteen plans using CC13 and CC01 ion chamber in Lucy phantom.	48
Table 4.7 The mean and range of percent point dose differences between measured dose and calculated dose and statistically significant differences of point dose difference between two systems. Differences are considered statistically significant for p-values < 0.05.	48
Table 4.8 The percent gamma pass of fifteen plans using diode array detector in ArcCHECK and EBT3 film in Lucy phantom.	49
Table 4.9 The mean and range of percent gamma pass between measured dose and calculated dose and statistically significant differences of gamma pass between two systems. Differences are considered statistically significant for p-values < 0.05.	51

Table 5.1 The comparison of percent point dose difference between this study, Ryan et al. and Parmider et al. studies.	53
Table 5.2 The percent gamma pass, measured dose and calculated dose of fifteen plans using EBT3 film in Lucy phantom.	54
Table 5.3 The comparison of the mean of percent gamma pass using diode array detector in ArcCHECK between this study, Christian et al. and Vibbha et al. study.	55
Table 5.4 The comparison of the mean of percent gamma pass using EBT3 film in different phantoms between this study Davide et al and Jin-Beom et al. study.	55



LIST OF FIGURES

Figure 2.1 The Gamma Knife machine treatment.....	6
Figure 2.2 The stereotactic radiosurgery with a Linac machine.	7
Figure 2.3 The CyberKnife machine.....	7
Figure 2.4 The proton machine.	8
Figure 2.5 The lung cancer with three dimensional conformal radiation therapy techniques.	10
Figure 2.6 The lung cancer with intensity modulated radiation therapy techniques. .	11
Figure 2.7 The lung cancer with Volumetric modulated arc therapy techniques.	12
Figure 2.8 (a) The beam profile without and (b) with flattening filter.	14
Figure 2.9 The geometric representation of dose distribution evaluation criteria using the combined ellipsoidal dose-difference and distance-to-agreement tests. (a) Two-dimensional representation. (b) One-dimensional representation.	17
Figure 2.10 The ionization chamber (IBA CC01 ion chamber).	18
Figure 2.11 The ArcCHECK (diode array detector).....	18
Figure 2.12 (a) The Gafchromic EBT3 film and (b) structure of Gafchromic EBT3 film.	20
Figure 3.1 Research design model.	23
Figure 3.2 Conceptual frameworks.	24
Figure 3.3 The Varian TrueBeam™ linear accelerator.....	25
Figure 3.4 The virtual water slab phantom.	26

Figure 3.5 The 3D diode array detector (ArcCHECK).....	26
Figure 3.6 The Lucy 3D QA phantom.	27
Figure 3.7 (a) The ionization chamber of 0.01 cc and (b) 0.13 cc ion chamber.	27
Figure 3.8 The Dose-1 electrometer.	28
Figure 3.9 The Gafchromic EBT3 film.....	28
Figure 3.10 The film scanner (Epson perfection v700 photo).	29
Figure 3.11 The eclipse Treatment Planning System.	30
Figure 3.12 The SNC patient software.....	30
Figure 3.13 (a) The 2×2 cm ² EBT3 film and (b) film calibration setting up in virtual slab phantom.....	31
Figure 3.14 The dose calibration of detector diode array (ArcCHECK).....	32
Figure 3.15 The VMAT QA plans for CC13 in ArcCHECK phantom.	33
Figure 3.16 The VMAT QA plans for CC13 in Lucy phantom.....	33
Figure 3.17 The VMAT QA plans for CC01 in Lucy phantom.....	34
Figure 3.18 (a) The CC13 ion chamber inserted in ArcCHECK front view and (b) side view.	34
Figure 3.19 The CC13 ion chamber inserted in Lucy phantom.....	35
Figure 3.20 The CC01 ion chamber inserted in Lucy phantom.....	35
Figure 3.21 The Dose-1 electrometer with +300 volt.....	36
Figure 3.22 The VMAT QA plans for ArcCHECK phantom.....	37

Figure 3.23 The VMAT QA plans for EBT3 film in Lucy phantom.....	37
Figure 3.24 The EBT3 film inserted in Lucy phantom.....	38
Figure 3.25 The EBT3 film reading by Epson film scanner.....	38
Figure 3.26 The comparison between measured dose and calculated dose using SNC patient software for ArcCHECK.....	40
Figure 3.27 The comparison between measured dose and calculated dose using SNC patient software for EBT3 film.....	40
Figure 3.28 The certificate of Approval from Ethic Committee of Faculty of Medicine Chulalongkorn University.....	42
Figure 4.1 The film calibration curve between absorbed dose and pixel value.....	44
Figure 4.2 The scatter plot of percent point dose difference of fifteen plans using CC13 ion chamber in ArcCHECK.....	45
Figure 4.3 The scatter plot of percent point dose difference of fifteen plans using CC01 and CC13 ion chamber in Lucy phantom.....	47
Figure 4.4 The scatter plot of percent gamma pass of fifteen plans using diode array detector in ArcCHECK.....	50
Figure 4.5 The scatter plot of percent gamma pass of fifteen plans using EBT3 film in Lucy phantom.....	50

LIST OF ABBREVIATIONS

Abbreviation Terms

3D	Three dimensional
cGy	Centigray
CRT	Conformal radiation therapy
D	Dose
FFF	Flattening filter free
Fr	Fraction
Gy	Gray
IMAT	Intensity modulated arc therapy
IMRT	Intensity modulated radiation therapy
K_{TP}	Factor to correction for temperature pressure to the standard condition of calibration laboratory
K_{Q,Q_0}	Correction factor for beam quality
LINAC	Linear accelerator
M	Reading of dosimeter
MeV	Mega electron voltage
MLC	Multileaf collimator
MU	Monitor unit
MV	Megavoltage
N_{D,w,Q_0}	Calibration factor
nC	Nano coulomb
NSCLC	Non-small cell lung cancer
OD	Optical density
QA	Quality assurance

SABR	Stereotactic ablative radiotherapy
SAD	Source to axis distance
SBRT	Stereotactic body radiation therapy
SCLC	Small cell lung cancer
SRS	Stereotactic radiosurgery
SRT	Stereotactic radiotherapy
VMAT	Volumetric modulated arc therapy



CHAPTER I

INTRODUCTION

1.1 Background and rationale

The goal of radiotherapy is to apply high radiation to target or tumor cell and low radiation to normal tissue. The suitable treatment technique makes higher efficiency treatment. Nowadays, the treatment technique is developed to higher advance technique such as intensity modulated radiation therapy (IMRT), volumetric modulated arc therapy (VMAT), stereotactic radiosurgery (SRS), stereotactic radiotherapy (SRT) and stereotactic body radiation therapy (SBRT). The IMRT and VMAT are widely used in routine treatment. The IMRT is delivered from fixed beam angles in order to create a conformal dose distribution while spare surrounding healthy tissue through the use of multileaf collimators (MLC) [1]. The VMAT is delivered from intensity modulated fields that the radiation is delivered while the gantry rotates; dose rate varies and MLC moves following target or tumor shapes.

Stereotactic technique is widely used to increase efficiency in clinical treatment. The technique of delivery a single fraction and high dose radiation therapy for treating intracranial lesions is called stereotactic radiosurgery (SRS). The delivery of high dose and multi dose fraction radiation therapy for treating intracranial lesions is called stereotactic radiotherapy (SRT).

In addition to stereotactic that is applied for treating intracranial, the technique applied for treating extracranial is stereotactic body radiation therapy (SBRT). The SBRT is delivered from a few fractions with large dose for treating small lesion in extracranial such as lung tumor.

To increase capability of treating, a flattening filter free (FFF) is applied with SBRT. Normally, a conventional technique uses flattening filter for uniformity intensity beams. For SBRT, the treating without a flattening filter free is more efficiency due to the short treatment time with using the high intensity of the real beams.

Patient specific quality assurance (QA) in radiotherapy is the process to ensure that the correct dose is delivered to the patient before the treatment process. The accuracy of dose delivery is important for advanced technique, so the QA of advance technique is needed before treating the patient. For high accuracy, the selection of dosimeters that are used for measurement is important. There are many dosimeters for using in QA such as ionization chambers, films, diode array detector etc. An ionization chamber is widely employed for absolute dose measurement. Film and diode array detector are suitable for relative dose measurement in 2 dimensions.

This study aims to compare the patient specific QA tools between two volume sizes of ionization chamber for point dose and between ArcCHECK and Gafchromic film in Lucy phantom for dose distribution in VMAT lung SBRT using unflattened photon beams.

1.2 Research objectives

To determine the different patient specific QA tool between two volume sizes of 0.01 and 0.13 CC ion chamber for point dose and between diode array detector in ArcCHECK and Gafchromic film in Lucy phantom for dose distribution in VMAT lung SBRT using unflattened photon beams.



CHAPTER II

REVIEW OF RELATED LITERATURES

2.1 Theories

2.1.1 Stereotactic technique

Stereotactic is the treatment technique that delivered high dose with single or multi fraction radiation in small target volume. The technique can be divided by treatment region to two types. The one is stereotactic for treating intracranial and another one is stereotactic for treating extracranial.

2.1.1.1 Stereotactic for treating intracranial lesions

- Stereotactic radiosurgery (SRS) is a non-surgical procedure that is a single fraction radiation therapy with a high dose for treating intracranial lesions using a combination of a stereotactic apparatus and narrow multiple beams delivered through noncoplanar isocentric arcs.

Radiosurgery was coined by a neurosurgeon Lars Leksell in 1951. He developed the procedure in the late 1940s to destroy dysfunctional loci in the brain using orthovoltage x-ray and particle accelerators. Heavy charged particles, gamma rays, and megavoltage x rays have been used in the intervening decades to irradiate arteriovenous malformations as well as benign and malignant tumors.[2].

- Stereotactic radiotherapy (SRT) is a multiple dose fractions radiation therapy in commonly 2-5 fractions with a high dose for treating intracranial lesions.

SRS and SRT are essentially two-step processes consisting of: (1) accurately defining the shape and location of the lesion and the neuroanatomical in the reference frame of a stereotactic frame system with CT, MRI or angiography; and (2) developing and delivering the planned treatment. The treatment techniques produce a concentrated dose in the lesion with steep dose gradients external to the treatment volume. The rapid dose falloff from the edge of the treatment volume provides dramatic sparing of normal brain tissues.

Accuracy limits not only reflect the technical limitations of the frames and treatment units, but also reflect the current knowledge of the neurological abnormality and its radiation response. Two SRS techniques report uncertainties in target alignment with the beam focus of 0.2-0.4 mm in patient position, whereas the linac setup uncertainty is 1.0 mm [3]. Although the techniques differ in accuracy, it is unclear whether the difference is clinically significant. The uncertainty in dose delivery is a result of two processes: (1) target definition and (2) the machine tolerances of the dose delivery apparatus (including the frame). A reasonable

perspective on accuracy requirements for SRS should include (1) the current accuracy in external beam therapy; (2) the net result of uncertainties in SRS; (3) the resolution of the target image; and (4) the relationship of the image to the lesion itself, macroscopic and microscopic.

SRS has several advantages for cancer treatment:

- It can target tumors anywhere in the brain.
- It spares normal tissue near the tumor.
- It offers treatment for patients who would not do well with surgery.
- It requires fewer treatment fractions compared with traditional radiation therapy, patients may receive 10 or more treatments over several weeks.

2.1.1.2 Stereotactic for treating extracranial lesions

Stereotactic body radiation therapy (SBRT) [1]

Over 4000 publications spanning several decades have affirmed the clinical usefulness of stereotactic radiosurgery (SRS) in the treatment of benign and malignant lesion, as well as functional disorders. The radiobiological rationale for SBRT is similar to that for SRS; delivering a few fractions of large dose in relatively short overall treatment time results in a more potent biological effect. The clinical outcome of SBRT for both primary and metastatic diseases compare favorably to surgery with minimal adverse effect. In addition, the limited number of treatment fractions makes SBRT more convenient for patient and potential more cost-effective treatment modality than traditional radiation therapy.

Clinical patient outcomes for SBRT were first published in 1995 [4]. In Germany, investigators initially focused on the treatment of liver and lung lesions. In the United States, the first publications described the treatment of lung tumors. Prospective Phase I and/or II trials were published in 2001 for the treatment of lung and, in 2003, for liver. The RTOG has completed enrollment of a Phase II study of SBRT for medically inoperable primary non-small-cell lung cancer (NSCLC). Outcomes of retrospective series treating spinal lesions were first published in 2003 [5].

Stereotactic body radiation therapy (SBRT) refers to an emerging radiotherapy procedure that is highly effective in controlling early stage primary and oligometastatic cancers at locations throughout the abdominopelvic and thoracic cavities, and at spinal and paraspinal sites. The feature of SBRT is the delivery of large doses in a few fractions, which results in a high biological effective dose (BED). In order to minimize the normal tissue toxicity, conformation of high doses to the target and rapid fall-off doses away from the target is critical. The comparison of characteristics of 3D, IMRT and SBRT is shown in table 2.1.

Table 2.1 The comparison of typical characteristics of 3D/IMRT radiotherapy and SBRT[1].

Characteristic	3D/IMRT	SBRT
Dose/fraction	1.8-3 Gy	6-30 Gy
No. of fraction	10-30	1-5
Target definition	CTV/PTV (gross disease + clinical extension); Tumor may not have a sharp boundary.	GTV/CTV/ITV/PTV (well-defined tumors: GTV=CTV)
Margin	Centimeters	Millimeters
Physics/dosimetry monitoring	Indirect	Direct
Required setup accuracy	TG40,TG142	TG40,TG142
Primary imaging modalities used for treatment planning	CT	Multimodality: CT/MR/PET-CT
Redundancy in geometric verification	No	Yes
Maintenance of high spatial targeting accuracy for the entire treatment	Moderately enforced (moderate patient position control and monitoring)	Strictly enforce (sufficient immobilization and high frequency position monitoring through integrated image guidance)
Need for respiratory motion management	Moderate-Must be at least considered	Highest
Staff training	Highest	Highest + special SBRT training
Technology implementation	Highest	Highest
Interaction with systemic therapies	Yes	Yes

SBRT has been under increasing study because of various advantages over conventional radiotherapy. The advantages of hypo fractionated radiotherapy for treating bone metastases include a shortened treatment course and the ability to irradiate a smaller normal tissue volume because of rapid dose fall-off on SBRT treatment plans when compared to standard multi fractionated radiotherapy. Possibly the largest advantage is the ability to deliver an ablative dose without incurring previously dose-limiting tissue toxicity. SBRT may also provide faster and more durable pain relief. The delivery of a biologically more potent dose may provide better local control. Because of this large dose delivery, radio resistant tumors such as melanoma, renal cell carcinoma, and sarcoma, which tend to metastasize to the bone, can now be investigated as viable treatment targets. Similarly, the treatment of

previously irradiated sites with SBRT can now be investigated due to the increased accuracy and reduced treatment volumes of SBRT over conventional therapy.

On the other hand, SBRT comes with its own unique disadvantages as well. To achieve the increased accuracy with the use of immobilization devices, image guidance, multiple beams, intensity-modulated beam delivery or a combination of any of these, treatment times are increased as compared to conventional treatment. In the case of painful bone metastases, this increased time and planning/-delivery requirements can be difficult for the patient to bear. Some patients may require pretreatment pain medication or generalized anesthesia.

Additionally, if accuracy is compromised, surrounding tissues will receive high doses of radiation that could potentially lead to more severe toxicity after treatment. In the setting of spinal metastases, the surrounding critical normal tissues that can receive toxic doses include the spinal cord, small bowel, and respiratory tract structures. The doses to these serially functioning tissues are important to consider with the use of SBRT, because even if a small segment becomes damaged, the entire organ becomes nonfunctional. Some consider this to be the principle limiting factor in the use of SBRT.

Nowadays, there are several types of radiation used in SRS /SRT or SBRT.

- **Gamma Knife:** a machine is shown in figure 2.1, the precisely focuses about 201 beams of gamma radiation is emitted by Cobalt-60 sources, at malignant and nonmalignant brain tumors. It is usually given as a single high-dose treatment.

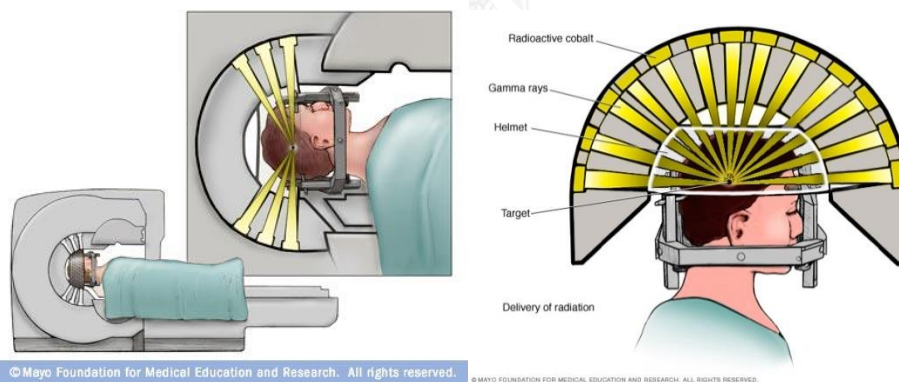


Figure 2.1 The Gamma Knife machine treatment.

- **Linear accelerator (LINAC):** a machine that uses X-rays (photons) to treat tumors in the brain and other parts of the body as shown in figure 2.2. The benefit of this technology is its ability to easily treat large tumor volumes (over 3.5 cm) for all body part by treating over several sessions. These machines can be performed SRS in a single session or over two to five sessions for larger tumors, which is called fractionated stereotactic radiotherapy.

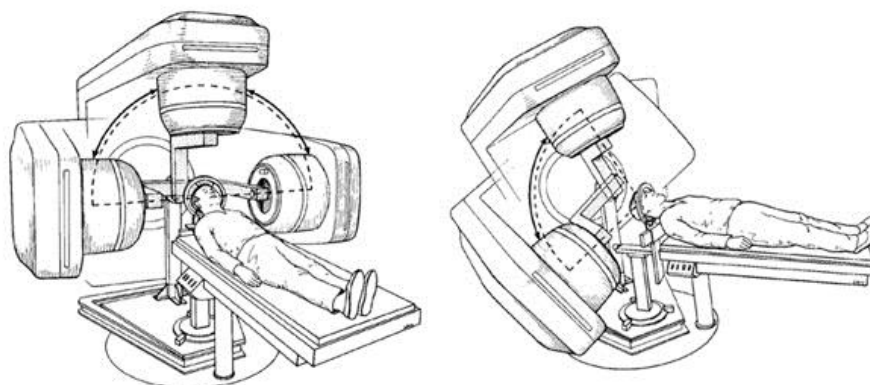


Figure 2.2 The stereotactic radiosurgery with a Linac machine.

- **CyberKnife:** It is a machine that is an advanced type of linear accelerator. A robotic system points the linear accelerator in a variety of positions. Several x-ray cameras (or imaging devices) and computers are used to track the person's position, the machine is shown in figure 2.3. If a person moves slightly, the robotic system can adjust by repositioning the linear accelerator before the beam of radiation is delivered. This machine is normally used to treat brain tumors.

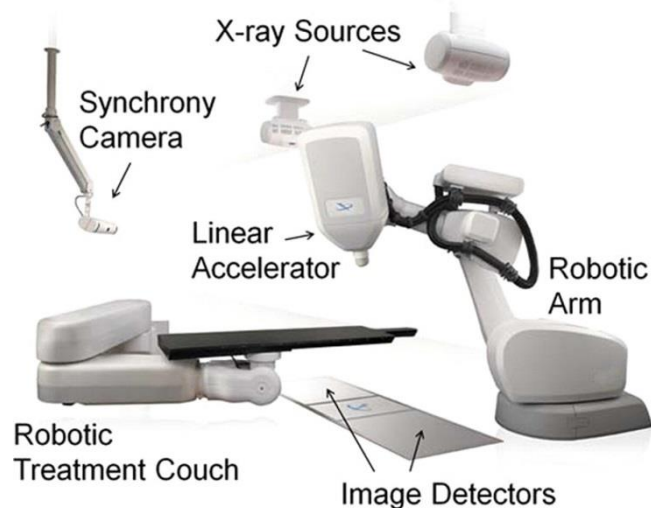


Figure 2.3 The CyberKnife machine.

- **Proton beam:** It is the highest advanced type of stereotactic radiosurgery. It can treat brain cancers in a single session using stereotactic radiosurgery or fractionated stereotactic radiotherapy to treat body tumors over several sessions. The machine is shown in figure 2.4.



Figure 2.4 The proton machine.

2.1.2 Volumetric modulated arc therapy (VMAT)

The development of intensity-modulated radiotherapy (IMRT) has greatly advanced the field of radiation oncology since its introduction to the clinic in 1990s. Since then, IMRT has been widely used to treat different types of cancers. It is capable of modulating the intensity of the radiation fields such that the tumor is adequately covered while the dose to healthy tissue is minimized.

In 1995, Yu [6] proposed the linac-based rotating cone-beam technique, and called this technique intensity-modulated arc therapy (IMAT) as an alternative to tomotherapy. In the original design of IMAT, several arcs were required to achieve intensity modulation.

One key feature of IMRT is inverse planning, where computational optimization algorithms are utilized to design the motion trajectories or segment shapes of the MLC to achieve intensity modulation. Depending on the planning technique, the MLC patterns can be directly outputted by the optimization algorithm, or be converted from the optimized fluence map with a leaf-sequencing algorithm. Different planning systems and optimization algorithms have been developed for static gantry IMRT. At that time, an efficient planning method for IMAT was not available, yet much research has since been devoted to developing optimization algorithms for IMAT. In 2008, Otto designed an optimization algorithm to deliver IMAT in a single-arc manner, which he called volumetric-modulated arc therapy (VMAT). In VMAT delivery, both dose rate and gantry rotation speed can be varied. These additional degrees-of-freedom increased the capability of beam intensity modulation [7].

VMAT is the advance treatment technique that is a specific type of intensity-modulated radiation therapy (IMRT) in which the gantry speed, multileaf collimator (MLC) leaf position and dose rate vary continuously during delivery. VMAT can potentially deliver a radiation field that better conforms to the tumor volume while reducing treatment time [8].

On Varian machines (Palo Alto, CA, USA), VMAT is referred to as RapidArc, while on Elekta machines, it is simply called VMAT. RapidArc® Radiotherapy Technology is an advanced form of IMRT that delivers a precisely-sculpted 3D dose distribution with a 360-degree rotation of the gantry in a single or multi-arc treatment. Unlike conventional IMRT treatments, during which the machine must rotate several times around the patient or make repeated stops and starts to treat the tumor from a number of different angles, RapidArc can deliver the dose to the entire tumor in a 360-degree rotation, typically in less than two minutes.

VMAT has several potential advantages over traditional methods of IMRT delivery. The main advantage is that treatments are delivered in a fraction of the time as compared with fixed beam IMRT treatments. Rao et al. [9] compared VMAT treatments with fixed-beam IMRT and helical tomotherapy treatments. VMAT treatment times varied from 2.1 to 4.6 minutes, IMRT treatment times varied from 7.9 to 11.1 minutes, and tomotherapy treatment times varied from 4.0 to 7.0 minutes. Other work has shown similar decreases in treatment time [10], [11]. The possible advantages of decreased treatment time include increased patient comfort and compliance, increased patient throughput, and enhanced image guidance.

Another advantage of VMAT is increased monitor unit (MU) efficiency, meaning fewer MUs are required to deliver the prescribed dose. Increased MU efficiency has two main effects: reducing the wear and tear on the treatment machine, and decreasing leakage and scatter dose. Rao et al. [9] found that the VMAT treatments they planned used 18% fewer monitor units than fixed-beam IMRT plans for the same geometries. Others have found similar increased MU efficiency for VMAT treatments [12].

Both decreased treatment time and increased MU efficiency have been achieved while maintaining target coverage and OAR sparing similar to fixed-beam IMRT. In some cases, VMAT has shown better OAR sparing than fixed-beam IMRT [9], [11], [12].

The main disadvantage of VMAT has been an increased optimization time as compared to fixed-beam IMRT [9]. However, optimization times have decreased, and as techniques develop, this disadvantage will continue to be mitigated.

2.1.3 Treatment technique for lung cancer

2.1.3.1 Lung cancer

There are two main types of lung cancer that have different microscopic appearances:

- Non-small-cell lung cancer (NSCLC) tends to grow more slowly and takes longer to spread beyond the lung. Local treatments such as surgery and/or radiation therapy are the mainstay of treatment for NSCLC. If chemotherapy is used, it is often to increase the effectiveness of surgery or radiotherapy, and is generally different in

NSCLC than in SCLC. Different types of chemotherapy may be used for different types of non-small cell lung cancer.

- Small-cell lung cancer (SCLC) is usually found in active or former cigarette smokers. Although SCLC is less common than the other type of lung cancer, it is a more aggressive tumor that is more likely to spread to other body sites. Chemotherapy is the mainstay of the treatment for SCLC. Radiation therapy is often used along with chemotherapy to treat lung tumors that have not spread beyond the chest or other organs. Surgery is not commonly used in SCLC due to its tendency to spread quickly. While surgery is seldom used to treat patients with SCLC, occasionally it is used to obtain tissue samples for microscopic study to determine the type of lung cancer present. For small cell lung cancer, after treatment directed to the disease in the chest, the radiation oncologist may suggest radiation therapy directed at the brain even though no cancer has been found there. This is called prophylactic cranial irradiation and is given to prevent lung cancer metastases from forming at this vital site.

2.1.3.2 Radiotherapy treatment technique for lung cancer

- Three-dimensional conformal radiation therapy (3D-CRT), which is shown in figure 2.5, combines multiple uniform radiation treatment fields to deliver precise doses of radiation to lung tumor.

The concept of conformal dose distribution has also been extended to include clinical objectives such as maximizing tumor control probability (TCP) and minimizing normal tissue complication probability (NTCP). Thus, the 3D-CRT technique encompasses both the physical and biologic rationales in achieving the desired clinical results.

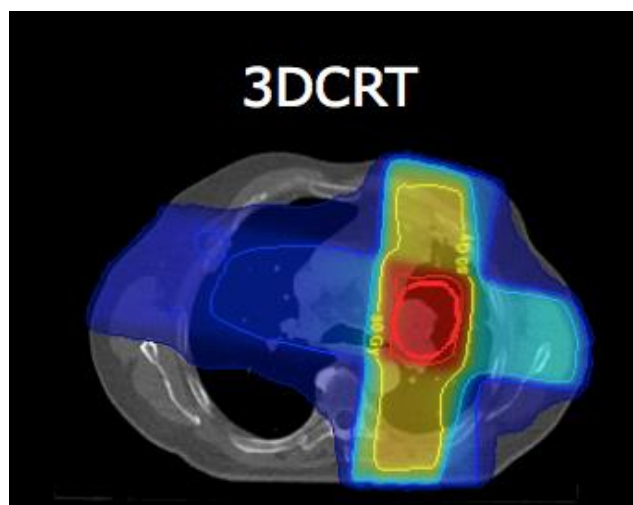


Figure 2.5 The lung cancer with three dimensional conformal radiation therapy techniques.

- Intensity modulated radiation therapy (IMRT), which is shown in figure 2.6, is an advanced form of 3D therapy. IMRT refers to a radiation therapy technique in which a non-uniform fluence is delivered to the patient from any given position of the treatment beam to optimize the composite dose distribution. The treatment criteria for plan optimization are specified by planner and the optimal fluence profiles for given set of beam direction are determined through “inverse planning”.

The principle of IMRT is to treat a patient from a number of different directions with beams of nonuniform fluences, which have been optimized to deliver a high dose to the target volume and an acceptably low dose to the surrounding normal structures. This technique is used most often if tumors are near important structures such as the spinal cord. Many cancer centers now use IMRT in lung cancer treatment.

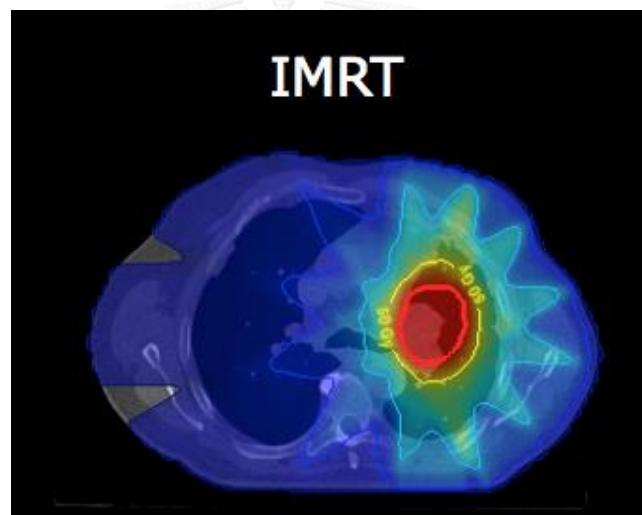


Figure 2.6 The lung cancer with intensity modulated radiation therapy techniques.

- Volumetric modulated arc therapy (VMAT), which is shown in figure 2.7, is a radiotherapy technique in which the gantry rotates while the beam is on. Multileaf collimator (MLC) position, dose rate and gantry vary continuously during the irradiation. VMAT can potentially deliver a radiation field that comparably conforms to the tumor volume compared with IMRT while reducing treatment time. The shorter treatment time of VMAT can increase patient throughput, reduce the risk of intrafraction motion (especially in lung), and improve patient comfort during treatment.

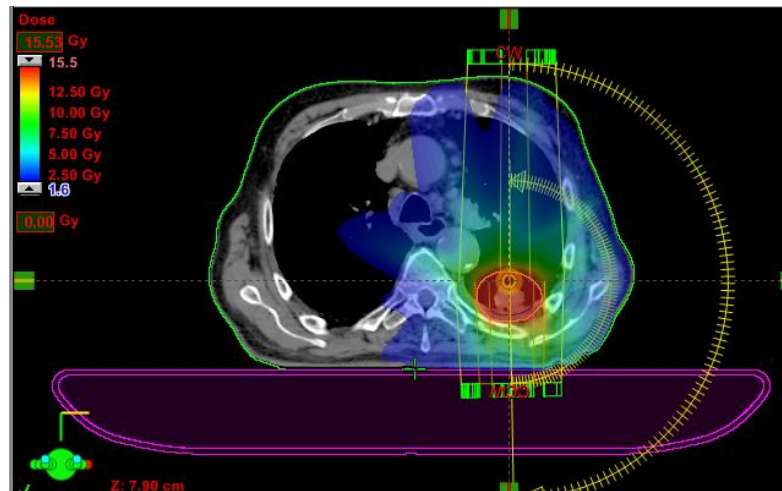


Figure 2.7 The lung cancer with Volumetric modulated arc therapy techniques.

- Stereotactic body radiation therapy (SBRT) also known as stereotactic ablative radiotherapy (SABR), is sometimes used to treat very early-stage lung cancers when surgery isn't an option due to a person's health or in people who don't want surgery.

Instead of giving a small dose of radiation each day for several weeks, SBRT uses very focused beams of high-dose radiation given in fewer (usually 1 to 5) treatments. Several beams are aimed at the tumor from different angles. To target the radiation precisely, patients are commonly put in a specially designed body frame for each treatment. This reduces the movement of the lung tumor during breathing. Like other forms of external radiation, the treatment itself is painless.

Early results with SBRT for smaller lung tumors have been very promising, and it seems to have a low risk of complications. It is also being studied for tumors that have spread to other parts of the body, such as the bones or liver.

2.1.4 Flattening filter free

Photon beams are generated by bombarding a high-Z target with a high energy electron beam. The resultant megavoltage bremsstrahlung beams present a bell-shape profile with high intensity at the center. In conventional linear accelerators, uniform intensity across the treatment field is obtained by placement of a flattening filter.

To increase capability for treatment, a flattening filter free (FFF) is applied with advance technique such as SBRT. The primary purpose of the FFF is to provide much higher dose rates available for treatments. For example, FFF X-rays from Varian TrueBeam can deliver 1400 MU/minute for 6 MV X-rays and 2400 MU/minutes for 10 MV X-rays. Higher dose rates have definite clinical benefits in organ motion management. For example, larger dose fractions can be delivered in a single breath-hold or gated portion of a breathing cycle. In SRS or SBRT treatments,

large MUs are often required and FFF X-ray beams can deliver these large MUs in much shorter “beam-on” time. With shorten treatment time, these FFF X-rays improve patient comfort and dose delivery accuracy.

The characteristic of FFF are high intensity at the center, bell shape beam profile (shown in figure 2.8), narrow penumbra, low out of field dose and low neutron contamination.

When removing the flattening filter, the beam characteristics change. The profile of the FFF beam becomes conical and has a softer spectrum. The effect of off axis softening, seen in flattened beams, is not as significant in unflattened beams. Due to the reduction of this effect the depth dose characteristics are almost constant throughout the entire field. This is also observed in that the shape of the dose profile with depth changes less than for flattened beams (by only a few percentage units). Further, there is less head scatter when the flattening filter, being one of the main sources of scatter, is removed which might reduce the relative risk of out-of-field secondary malignancies. Finally, the fact that the maximum available dose rate is at least double the one in flattened beams is beneficial in reducing the duration of the treatment delivery [13].

FFF beams have many distinct characteristics compared to conventional photon beams. They have a difference maximum dose rate, beam intensity, beam profile, penumbra, out of field dose and neutron contamination which following in table 2.2.

Table 2.2 The different characteristics between with and without flattening filter of Varian TrueBeam.

	With flattening filter	Flattening filter free
Maximum dose rate	600 MU/min	1,400 MU/min (6 MV) 2,400 MU/min (10 MV)
Beam intensity	Uniform beam intensity	Highest intensity at the center
Beam profile	A flatten beam profile	A bell shape beam profile
Penumbra	Wide	Narrow
Out of field dose	High	Low
Neutron contamination	High	Low

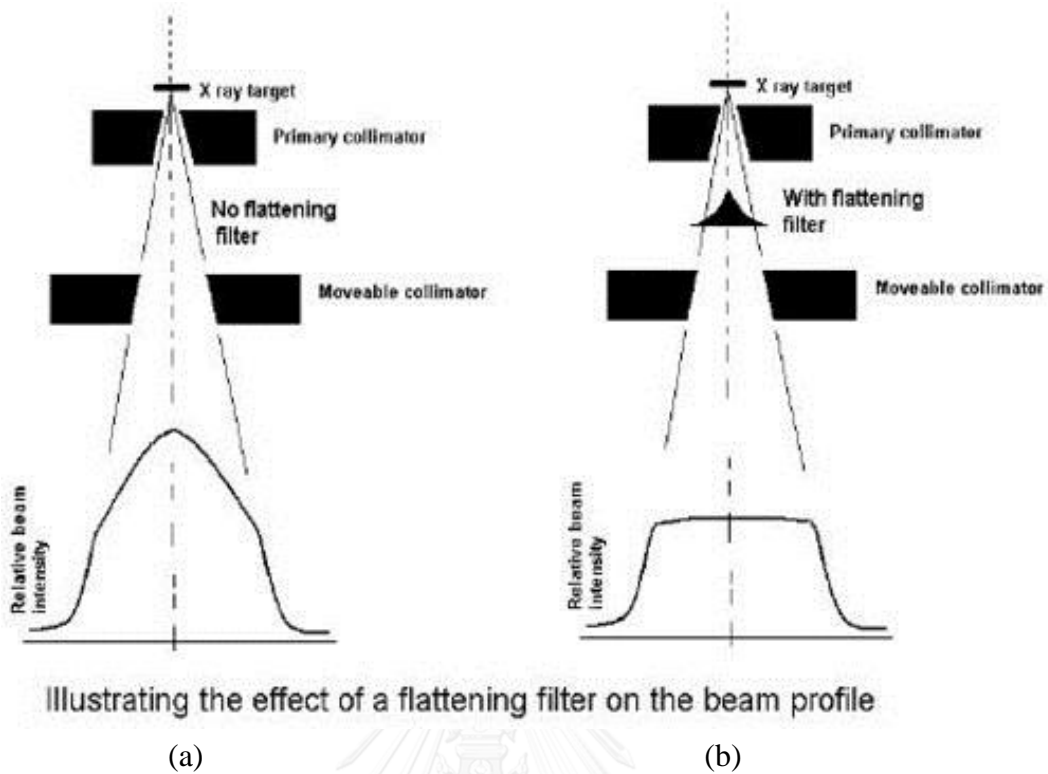


Figure 2.8 (a) The beam profile without and (b) with flattening filter.

2.1.5 Patient specific quality assurance

Since, the treatment is developed to advance treatment technique such as VMAT technique. So for quality assurance, the pre-treatment verification or patient specific QA needed to be performed.

Quality assurance (QA) in radiation therapy is the method used to ensure that the correct amount of radiation is being delivered to the correct location. QA is performed routinely on all parts of the treatment process, from planning to delivery. The QA performed on traditional treatments tends to consist of testing the capabilities of the system. For example, the flatness and symmetry of the beam are measured to ensure they are within predetermined tolerances. When a system is found to be within these tolerances, traditional treatments are generally delivered without further testing of the individual plans, because the possible errors are few and are quantifiable [14].

Patient specific QA is the procedure of verification to ensure that each individual patient's treatment plan conforms to the establish protocols and is delivered as planned. The purposes of patient specific QA are MLC position checking and verify a calculated dose for the planned treatment.

The most accurate QA possible would be performed by taking dosimetric measurements inside of the patient during the treatment delivery. However, this is not a practical method. Instead, treatment plans are typically copied onto a phantom geometry in which dosimetric measurements can be taken. The treatment is delivered to the phantom and measured doses are compared to calculated doses from the

treatment planning system. The assumption is made that if the planning system can accurately predict the dose to a phantom, it can also accurately predict the dose to a patient.

Patient specific QA procedure can be categorized from 1D to 3D verification. One dimensional verification carried out with single point detector system such as ionization chamber. It has excellent stability, linear response to absorbed radiation, small directional dependence and beam quality response independence. Measurement with ionization chamber results average dose over the whole volume.

Higher complexity of dose calculation in the treatment planning system of VMAT and also accuracy and reproducibility in delivery of VMAT plans need higher precision of verification method. So 2D (planes) and 3D (volumes) verification methods play an important role in QA procedure.

Devices with detector arrays and also films (radiographic or radiochromic film) can provide 2D information for dose measurements. The dose distribution is measured on a plane perpendicular to the central axis of the beam. Two dimensional detectors give good spatial resolution, fast response and easy analysis of the measured data.

Three dimensional dose distribution measurements can be done using film or cylindrical array detectors, such as OCTAVIUS, ArcCHECK, by rotating the gantry.

2.1.6 Plan evaluation

There are several methods used to evaluate quality of plan such as the percent point dose difference and gamma evaluation method.

2.1.6.1 The percent point dose difference

For point dosimetry, the percent point dose difference between calculated and measured doses is used for plan evaluation, The QA result will pass if the percent difference is within criteria such as 3% [15]. Point dose is analyzed using the following formula:

$$\% \text{ Point dose difference} = \frac{\text{Calculated dose} - \text{Measured dose}}{\text{Measured dose}} \times 100\% \dots\dots\dots (2.1)$$

2.1.6.2 Gamma evaluation method [16]

The gamma evaluation method has been used for patient specific quality assurance procedure in 2 or 3 dimensional. The gamma tool is developed to quantitatively compare dose distribution. The commissioning of a treatment planning system requires comparisons of measured and calculated dose distributions.

Quantitative evaluation methods directly compare the measured and calculated dose distribution values. Van Dyk et al. [17] described the quality assurance procedures of treatment planning systems and subdivide the dose distribution

comparisons into regions of high and low dose gradients, each with a different acceptance criterion. In low gradient regions the doses are compared directly, with an acceptance tolerance placed on the difference between the measured and calculated doses. Visualization of the dose difference distribution identifies region of disagreement. Because the dose difference in high dose regions may be misleading, Van Dyk et al. used the concept of DTA. The DTA is the distance difference between a measured data point and the nearest point in the calculated dose distribution that exhibits the same dose. The dose-difference and DTA evaluations complement each other when used as determinants of dose distribution calculation quality.

The determination of acceptance criteria is considered by an ellipsoid, which is shown in figure 2.9, at the surface. The equation defining the surface is

$$1 = \sqrt{\frac{r^2(r_m, r)}{\Delta d_M^2} + \frac{\delta^2(r_m, r)}{\Delta D_M^2}} \dots\dots\dots (2.2)$$

Where

$(r_m, r) = |r - r_m|$ is the distance between the reference and compared point.

$\delta(r_m, r) = D(r) - D_m(r_m)$ is the dose difference at the position r_m .

The quality on the right-hand side of equation 2.1 can be used to identify index γ at each point in the evaluation plan $r_c - r_m$ for the measurement point r_m ,

$$\gamma r_m = \min \{ \Gamma(r_m, r_c) \} \forall (r_c) \dots\dots\dots (2.3)$$

where

$$\Gamma(r_m, r_c) = \sqrt{\frac{r^2(r_m, r_c)}{\Delta d_M^2} + \frac{\delta^2(r_m, r_c)}{\Delta D_M^2}} \dots\dots\dots (2.4)$$

$$r(r_m, r_c) = |r_c - r_m| \dots\dots\dots (2.5)$$

and

$$\delta(r_m, r_c) = D_c(r_c) - D_m(r_m) \dots\dots\dots (2.6)$$

is the difference between dose values on the calculated and measured distributions, respectively. The pass-fail criteria therefore become

$\gamma(r_m) \leq 1$, calculation passes,

$\gamma(r_m) > 1$, calculation fails.

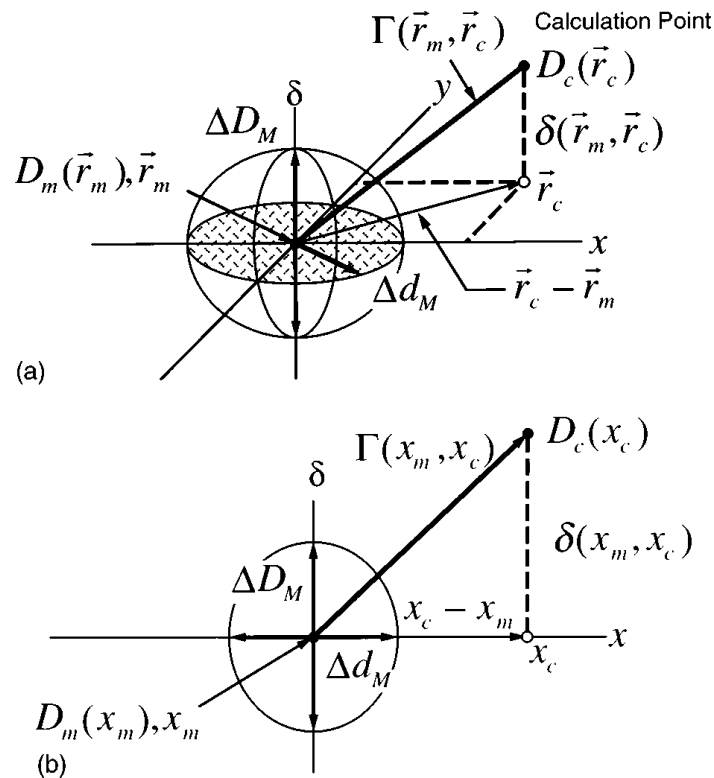


Figure 2.9 The geometric representation of dose distribution evaluation criteria using the combined ellipsoidal dose-difference and distance-to-agreement tests. (a) Two-dimensional representation. (b) One-dimensional representation.

2.1.7 Dosimeter

There are several dosimeters to use in patient specific QA. Each dosimeter has different property.

2.1.7.1 Ionization chamber

The ionization chamber, which is shown in figure 2.10, is widely performed in point dose measurement, because they are independence of energy, dose and dose rate. They provide a reproducible direct reading and can be calibrated to a national standard to calculate the dose. The ion chambers are various sizes that depend on suitable usage.

The IBA CC01 (IBA Dosimetry, Schwarzenbruck, Germany) is the conventional ionization chambers for measurements of small fields and of ranges with high dose gradients, e.g. stereotactic fields. The CC01 had an active volume of 0.01 cm^3 , an inner steel electrode, and an outer electrode made of Shonka plastic with 2-mm inner diameter and a 0.5-mm wall thickness. The diameter and length of the inner electrode were 0.35 and 2.8 mm, respectively. The reference point without the build-up cap was 2.3 mm from the distal end of the chamber thimble [18].

The IBA CC13 (IBA Dosimetry, Schwarzenbruck, Germany), the standard chamber for clinical use in water phantoms and for output factor measurements. The CC13 had an active volume of 0.13 cm^3 , a cavity length of 5.8 mm, a cavity radius of 3.0 mm and a wall thickness of 0.07 g/cm^2 .



Figure 2.10 The ionization chamber (IBA CC01 ion chamber).

2.1.7.2 Diode array detector (ArcCHECK)

The ArcCHECK (Sun Nuclear Corporation, Melbourne, USA), which is shown in figure 2.11, is a cylindrical water equivalent phantom with a three-dimensional array of 1,386 detectors diode. The detector volume is 0.019 mm^3 . The diodes are placed between two layer of solid water or acrylic and spaced 1 cm apart. The detectors are embedded in a 2.85 cm linear depth of acrylic buildup that equivalent to 3.28 g/cm^3 density depth. All detectors are perpendicular to the beam for all gantry angles. The ArcCHECK is divided into two sections, which the inner section is 15 cm in diameter of acrylic insertion capable to insert a thimble ionization chamber for central axis dose measurement, if the inner section is removed, the accuracy of inhomogeneity correction of treatment planning can be checked. This device as no limit dose of measurement because each detector sensors are updated the measurement dose in every 50 ms. The ArcCHECK was designed specifically for rotational dosimetry. This device was used to verify the patient specific QA.



Figure 2.11 The ArcCHECK (diode array detector).

2.1.7.3 Radiochromic film [19]

Radiochromic effects involve the direct coloration of a material by the absorption of energetic radiation, without requiring latent chemical, optical, or thermal development or amplification.

The radiochromic reaction is a solid-state polymerization, whereby the films turn deep blue proportionately to radiation dose, due to progressive 1,4-trans additions which lead to colored polyconjugated, ladderlike polymer chains.

The radiochromic film, which is used for QA in this study, is a Gafchromic EBT3 film. The EBT-3 is designed for the measurement of absorbed doses of ionizing radiation. It is particularly suited for high-energy photons. The dynamic range of this film is designed for best performance in the dose range from 0.2 to 10 Gy, making it suitable for many applications in IMRT, VMAT and brachytherapy. For measurement of doses substantially greater than 10 Gy EBT-XD or MDV3 are preferred while the use of HD V2 is indicated for still higher dose measurement. The structure of EBT3 film is shown in Figure 2.12b. The film is comprised of an active layer, nominally 28 μm thick, sandwiched between two 125 μm matte-polyester substrates. The active layer contains the active component, a marker dye, stabilizers and other components giving the film its near energy independent response. The thickness of the active layer will vary slightly between different production lots. The Gafchromic EBT3 dosimetry film is made by laminating an active layer between two polyester layers as shown in figure 2.12b

Key technical features of Gafchromic EBT3 include:

- Dynamic dose range: 0.1 Gy to 20 Gy
- Optimum dose range: 0.2 Gy to 10 Gy, best suited for applications such as IMRT and VMAT
- Real time developing without post-exposure irradiation;
- Energy in-dependence: minimal response difference from 100keV into the MV range;
- Near tissue equivalent;
- High spatial resolution – can resolve features down to 25 μm , or less
- Proprietary new technology incorporating a marker dye in the active layer:
- Enables non-uniformity correction by using multi-channel dosimetry
- Decreases UV/visible light sensitivity;
- Stable at temperatures up to 60°C;

EBT3 dosimetry film can be handled in interior room light for short periods without noticeable effects. However, it is suggested that the film should not be left exposed to room light for hours, but rather should be kept in the dark when not in use. When the active component in EBT3 film is exposed to radiation, it reacts to form a blue colored polymer with absorption maxima at approximately 633 nm.

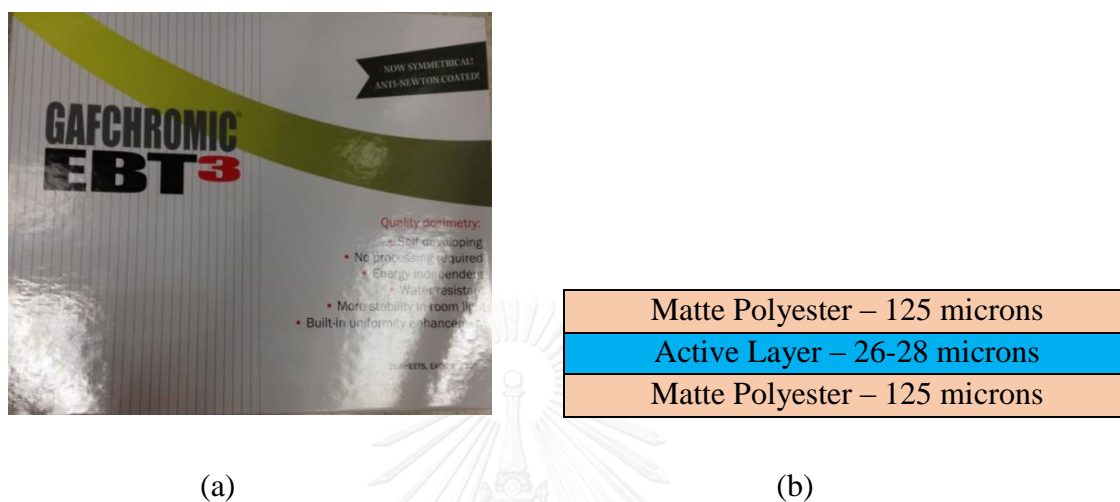


Figure 2.12 (a) The Gafchromic EBT3 film and (b) structure of Gafchromic EBT3 film.

2.2 Review of related literatures

Christian Ronn Hansen et al. [20] investigated the impact of FFF beams on VMAT treatment plan for lung SBRT treatments. A cohort of 21 consecutive patients with a dual arc technique for primary or metastatic tumors of the lung was selected. All patients were treated between January and May 2013 at Odense University Hospital, Denmark. Beams were delivered on the Versa HD linac which was equipped with two MLC banks each having 80 leaves with a projected width of 5 mm at iso-center. The maximum leaf speed is 6.5 cm/s. The plans were created using the Pinnacle treatment planning system. For each patient three plans were created: 1) dual VMAT arc FF beams (dFF) 2) dual VMAT arc FFF beams (dFFF) and 3) single VMAT arc FFF beams (dFFF). The actual beams on times were recorded. Dose distributions were measured using the Sun Nuclear ArcCHECK phantom and evaluated by a gamma analysis of 3%, 3 mm. Only detector readings above 10% of maximum dose were included in the pass rate evaluation. Pass rate above 95% were considered as clinically acceptable. The results were 99.3 %, 98.0 % and 98.0 % for dual FF, dual FFF and single FFF, respectively. The higher pass rate of dFF was statistically significant from the others two. All plans passed the 95% pass rate criteria and the detectors failing from the 3% and 3mm criteria were generally few and isolated. The treatment times were reduced significantly for the FFF treatments. For all patient, clinically acceptable plans were achievable and deliverable for both FF and FFF treatments. The plan quality for dual arc FF and FFF plans for SBRT lung produced in Pinnacle 9.2 and delivered on a Versa HD™ was equivalent.

Parminder Basran et al. [21] verified dosimetry of IMRT plans for stereotactic. All treatment plans were delivered with a 6 MV Siemens PRIMUS linear accelerator specifically adapted for stereotactic deliveries and intensity modulated radiation. The mechanical of the mMLC was 62 leaves, 10×12 cm filed size, 4.0 mm leaf width at isocenter and 2.5 cm/sec maximum leaf speed. The XPLAN RT2 Stereotactic Planning system (Radionics, Tyco Health Group LP, Burlington MA) is used to plan. The Absolute dosimetry was measured using a LUCY phantom (Sandstrom Trade and Techology Inc., Welland, Ontario) and PTW-31010 ion chamber (PTW-Frieburg Germany) with 2% tolerance. With the use of the LUCY phantom and applying appropriate correction factors, the LUCY phantom provides a convenient and efficient phantom for absolute dosimetry of complex IMRT plans. The ability to use the LUCY phantom for absolute dosimetry verification is particularly convenient since this phantom is routinely used for quantifying stereotactic localization errors. The discrepancy between measured and calculate doses was 0.9%. The practice was accepted a total absolute dose discrepancy $\pm 2.0\%$ for the ion chamber measurements. Larger errors from individual beams were accepted if the ion chamber volume was in a high dose-gradient region and providing that the cumulative dose from all beams remains within 2.0% of the prescribed dose.

Vibha Chaswal et al. [22] commissioned the ArcCHECK device under a strict comprehensive testing procedure, especially in consideration with the previous finds and upgrades, and investigated its usefulness for patient-specific VMAT QA. All measurements were done using the TrueBeam STx accelerator (Console version 1.6; Varian Medical Systems, Palo Alto, CA) with a 6 MV beam with and without flattening filter (denoted as 6X and 6F beam). Varian Eclipse treatment planning system (TPS) and analytical anisotropic algorithm (AAA) were used for calculating reference dose grids. TPS-calculated dose was used as the reference for ArcCHECK evaluation testing. The comparison of phantom-measured versus TPS-calculated dose was based on profiles and 3D gamma analysis. The global and local gamma indices (γ index) were both computed for 3 mm/3% and 2 mm/2% criterion using the SNC software. Gamma evaluations were performed in the absolute dose mode, with the default normalization to the maximum dose in the curved plane and a low-dose threshold of 10%. The results were 98.9% and 95.2% gamma passing rates at 3%/3mm and 2%/2mm for the unfiltered 6F beam, respectively. For the 6X beam, the average global γ (2%/2 mm) was slightly lower than 90% (1.4% lower), whereas γ (3%/3mm) was 96.06%. All the considered VMAT plans passed the clinically accepted QA pass criteria of γ (3%/3 mm) > 90%, for IMRT and VMAT plan QA.

Daide Cusumano et al. [23] examined the feasibility of using the new Gafchromic EBT3 film in a high-dose stereotactic radiosurgery and radiotherapy quality assurance procedure. A quality assurance (QA) dosimetric protocol was developed using Gafchromic EBT3 (batchnumber: AO4041203) in conjunction with the flatbed scanner Epson Expression 10000XL (SeikoEpsonCorp.,Nagano,Japan). This protocol was then optimized to evaluate dose distributions effectively delivered with a CyberKnife system, version 9.6 (Accuray, Sunnyvale, CA) in comparison with planned ones. In this study, dosimetric verification of dose distributions of radiosurgical clinical interest (up to 8 Gy) was performed. Calibration curve was used in a QA protocol to verify patient-specific dose distributions, delivered with a CyberKnife system. Clinically administered dose distributions were reported on an Easy Cube cubic phantom (SunNuclear,Mel-bourne,FL), maintaining both treatment beams ballistic and monitor units. A Gafchromic EBT3 film was inserted in the phantom between the 2 central slabs, oriented in the axial direction. A high-dose threshold level for analyses using this procedure was established evaluating the sensitivity of the irradiated films. Sensitivity was found to be of the order of centiGray for doses up to 6.2 Gy and decreasing for higher doses. The agreement between dose distributions was then evaluated for 13 patients using gamma analysis. Results obtained using Gamma test criteria of 5%/1 mm showed a pass rate of 94.3%. Gamma frequency parameters calculation for EBT3 films showed strongly depends on subtraction of unexposed film pixel values from irradiated ones. In the frame work of the described dosimetric procedure, EBT3 films proved to be effective in the verification of high doses delivered to lesions with complex shapes and adjacent to organs at risk.

CHAPTER III

RESEARCH METHODOLOGY

3.1 Research design

This study is a retrospective observational descriptive study research.

3.2 Research design model

The diagram is shown in figure 3.1.

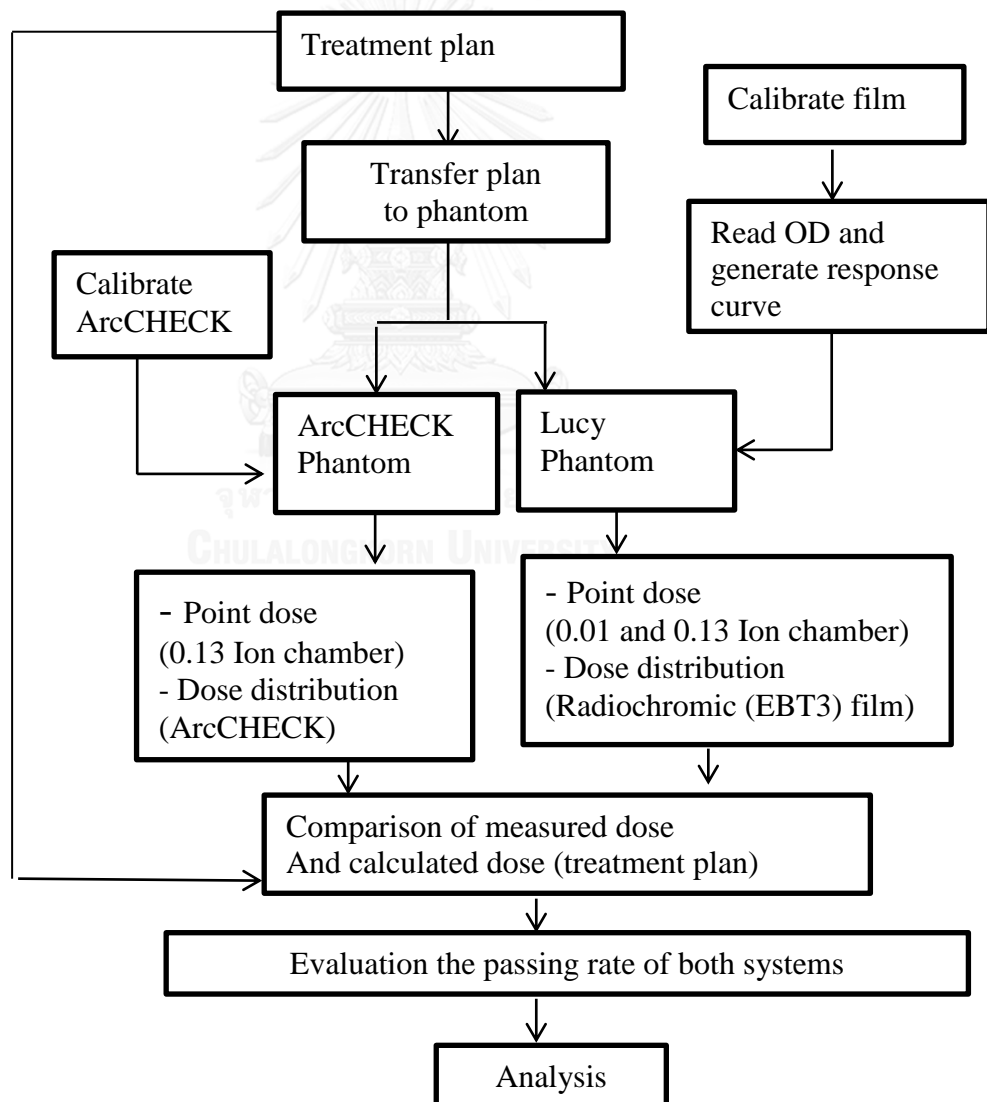


Figure 3.1 Research design model.

3.3 Conceptual frame works

The percent dose difference and gamma pass are affected by measured doses and calculated doses. The diagram of conceptual framework is shown in figure 3.2.

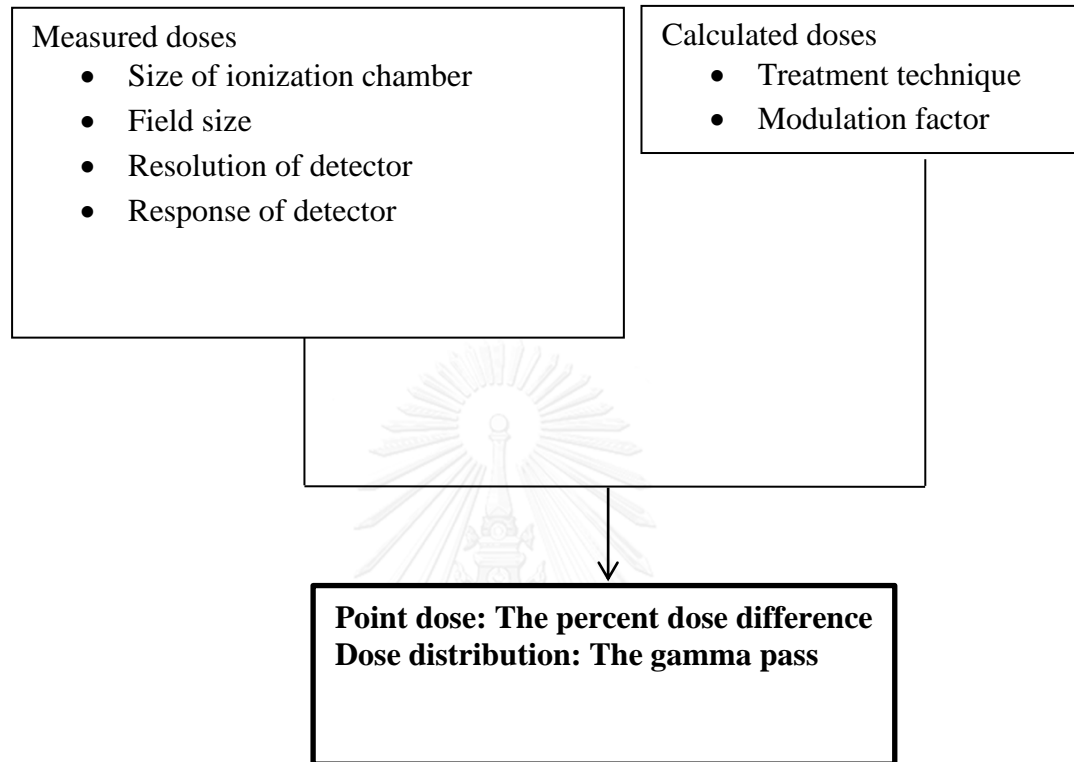


Figure 3.2 Conceptual frameworks.

3.4 Keyword

- Stereotactic body radiation therapy (SBRT)
- Flattening filter free (FFF)
- Patient specific quality assurance
- Dosimetry system

3.5 Research questions

3.5.1 Primary question

What is the difference in dosimetry for patient specific QA tools between ArcCHECK and Lucy phantom for VMAT SBRT using unflattened photon beams?

3.6 Materials

The materials used in this study were supplied from the Division of the Radiation Oncology, Department of Radiology, Faculty of Medicine, Chulalongkorn University.

3.6.1 Radiation beams

This study used Varian TrueBeam™ linear accelerator (Varian Medical system, Inc, Palo Alto, USA), as shown in figure 3.3, for beam radiation. This machine has photon beams of 6 MV, 10 MV, 6 MV (FFF), 10 MV (FFF) and six electron beam energies of 6, 9, 12, 15, 18 and 22 MeV. The maximum photon field size is 40×40 cm² at isocenter. The distance from the target to isocenter is 100 cm. The maximum dose rates are 600 MU/min for conventional mode, 1400 MU/min for 6XFFF high intensity mode and 2400MU/min for 10XFFF high intensity mode. The 6 MV (FFF) with maximum dose rates was used in this study.



Figure 3.3 The Varian TrueBeam™ linear accelerator.

3.6.2 Virtual water slab phantom

The virtual water slab phantom (GAMMEX RMI, Wisconsin, USA), which is shown in figure 3.4, is 1.03 g/cm^3 of the density and 5.97 of atomic number. It is made in square slab of $30 \times 30 \text{ cm}^2$ with the thickness of 0.2, 0.3, 0.5, 1.0, 2.0, 3.0, 4.0 and 5.0 cm. The property of virtual water phantom is investigated by comparing the dose measurement at the same thickness of virtual water slab phantom. This phantom was used for film calibration in this study.



Figure 3.4 The virtual water slab phantom.

3.6.3 ArcCHECK (3D diode array detector)

ArcCHECK (Sun Nuclear Inc, Melbourne, FL), which is shown in figure 3.5 was designed specifically for rotational delivery treatment technique. It utilizes unique cylindrical detector geometry. This system consists of 1386 diodes array which are embedded in the cylindrical wall of phantom. Each diode is $0.8 \times 0.8 \text{ mm}^2$ in the active area. The detector volume is 0.000019 cm^3 . It is about 21cm array diameter and length. The diodes are situated at depth of 2.85 cm acrylic build up and spaced 1 cm apart. It is built in rotation and tilt inclinometer, which is enable the calculation of gantry angle.

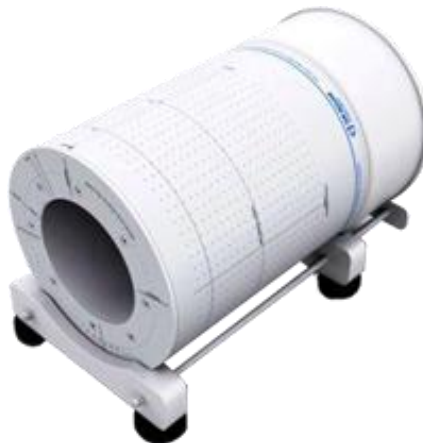


Figure 3.5 The 3D diode array detector (ArcCHECK).

3.6.4 Lucy 3D phantom

The Lucy 3D phantom (Sandström Trade and Technology Inc., Welland, Ontario, Canada), which is shown in figure 3.6, is tailored to provide the superior accuracy required for SRS QA. The Lucy is a highly precise phantom with tolerances of 0.1 mm. (Standard Imaging). The phantom has comprehensive QA package such as dosimetry insert for ion chamber and detector, target/treatment verification film cassette. In this study, the phantom was used with IBA CC01 and CC13 ionization chamber for point dose and EBT3 Gafchromic film for dose distribution measurement.

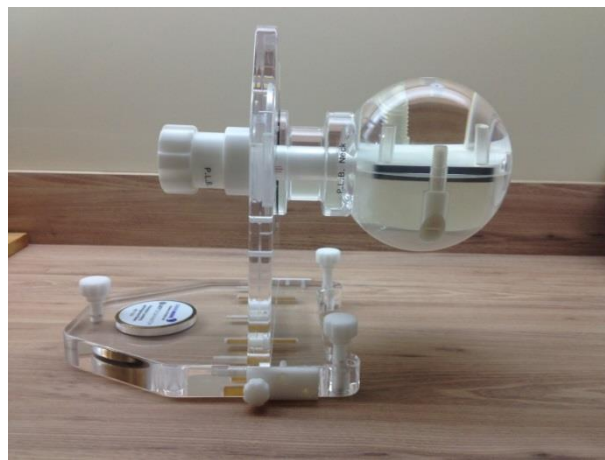


Figure 3.6 The Lucy 3D QA phantom.

3.6.5 The IBA 0.01 and 0.13 cc ionization chamber

The 0.01 and 0.13 cc ionization chamber (IBA Dosimetry, Schwarzenbruck, Germany), which are shown in figure 3.7 (a) and 3.7 (b), can measure absolute and relative dose of photon and electron beams in radiotherapy. In this study, the ionization chamber was inserted in ArcCHECK phantom and Lucy phantom.



(a)



(b)

Figure 3.7 (a) The ionization chamber of 0.01 cc and (b) 0.13 cc ion chamber.

3.6.6 Electrometer

The Dose-1 electrometer (IBA Dosimetry, Schwarzenbruck, Germany), which is shown in figure 3.8, is a high precision reference class electrometer that signification exceeds the recombination of the IEC 60731 and the AAPM ADLs. It is suitable to use with ionization chambers, semiconductors and diamond probes. This electrometer is employed with 0.01cc and 0.13 cc ionization chamber and set at +300 voltages.



Figure 3.8 The Dose-1 electrometer.

3.6.7 Gafchromic film

The 8×10 inch Gafchromic EBT3 film (Ashland Inc., Wayne, NJ, USA), which is shown in figure 3.9, is an ideal medium for quantitative dosimetry. The spatial resolution is better than 0.1 mm and the response is energy and fractionation independent. The EBT film is self-developing and can be handled in room light.

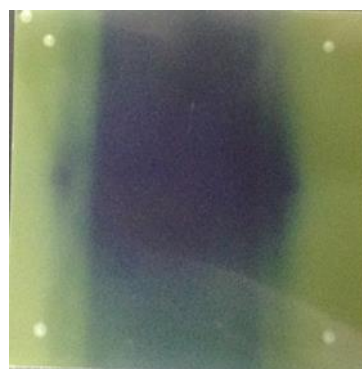
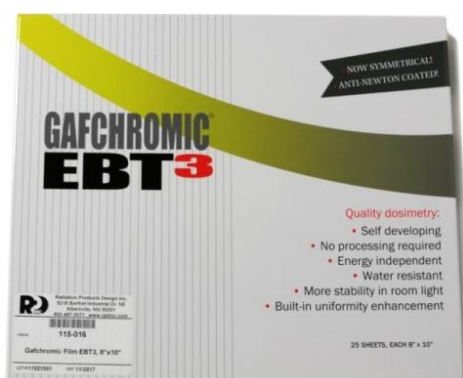


Figure 3.9 The Gafchromic EBT3 film.

3.6.8 Film scanner

The Epson Perfection V700 flat-bed color CCD (Epson America, Inc., USA), which is shown in figure 3.10, for EBT film digitization is used as a scanner. The maximum support of media size is 22×30 cm². The color depth of scanner is 48 bit color. The optical resolution of scanner is 6,400 dpi×9,600 dpi and the maximum resolution is 12,800 dpi×12,800 dpi of interpolated resolution.



Figure 3.10 The film scanner (Epson perfection v700 photo).

3.6.9 Eclipse Treatment Planning System

Eclipse treatment planning system version 11.0.31 (Varian medical Systems, CA, USA), which is shown in figure 3.11, is a treatment planning for all treatment technique such as 3D conformal, IMRT, VMAT, electron and brachytherapy. Eclipse version 11.0.31 provides the two photon dose calculation algorithms, Analytical Anisotropic Algorithm (AAA) and the new Acuros XB algorithm. Eclipse helps dosimetrists, physicists, and physicians efficiently create, select and verify the best treatment plans for patients.

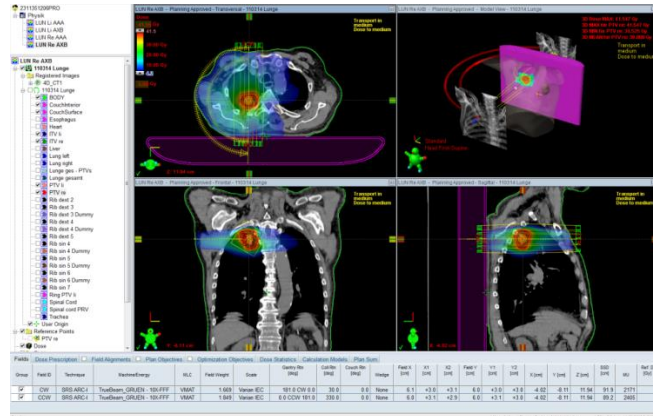


Figure 3.11 The eclipse Treatment Planning System.

3.6.10 Evaluation software

The ArcCHECK interface with SNC patient software, which is shown in figure 3.12, is a powerful and proven patient specific QA and analysis tool with over 2000 clinical installations. The same analysis and workflow options from MapCHECK® 2 are available in ArcCHECK. All data files from ArcCHECK are in an open format for easy export, including raw data. ArcCHECK QA plans are in three dimensions. DICOM RT Dose is imported and a 3D dose grid corresponding to detector locations is extracted for comparison to the measurement. The gamma criteria of 3%/3mm (dose difference and distance to agreement) is set for comparison.

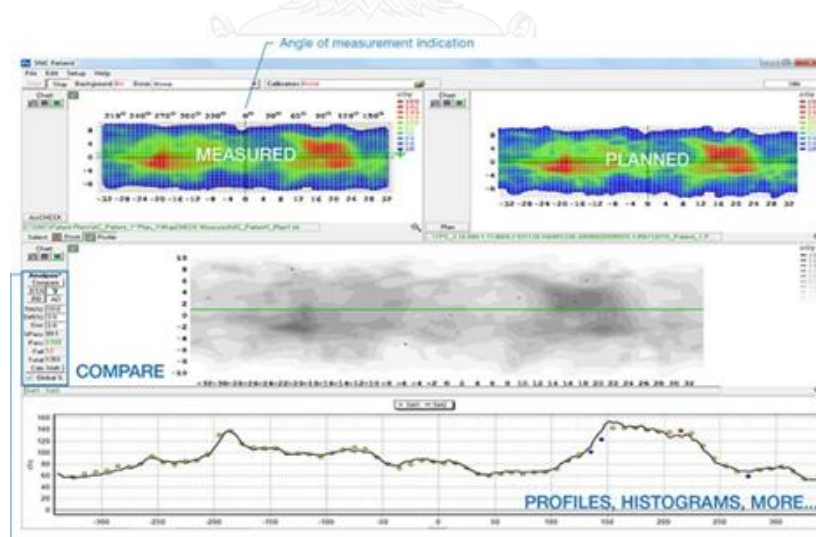


Figure 3.12 The SNC patient software.

3.7 Method

The 15 lung VMAT SBRT plans with 400-2500 cGy prescribed dose per fraction, 1-3 arc and 7.51-318.37 cm³ tumor volume from June 2016 to September 2016 at King Chulalongkorn Memorial Hospital were selected for this study. All measurements were performed with 6 MV FFF photon beams of 1,400 MU/min maximum dose rate from Varian TrueBeamTM linear accelerator. All plans were generated using the Varian Eclipse treatment planning system (version 11.0.31) with Acuros XB algorithm.

3.7.1 Film calibration

The Gafchromic EBT3 films which is shown in figure 3.13 (a) were cut into 2×2 cm² and inserted in Virtual slab water phantom, as shown in figure 3.13 (b) for 10×10 cm² field size at 7 cm depth, 100 SAD and 15 cm backscatter. The EBT3 were irradiated with 6 MV FFF beams of various doses (0, 200, 400, 800, 1000, 1500, 2000, 2500, 3000 and 4000 cGy) for 1,400 MU/min maximum dose rate. The optical density was read by an Epson Perfection V700 scanner with red channel and evaluated by SNC patient software.

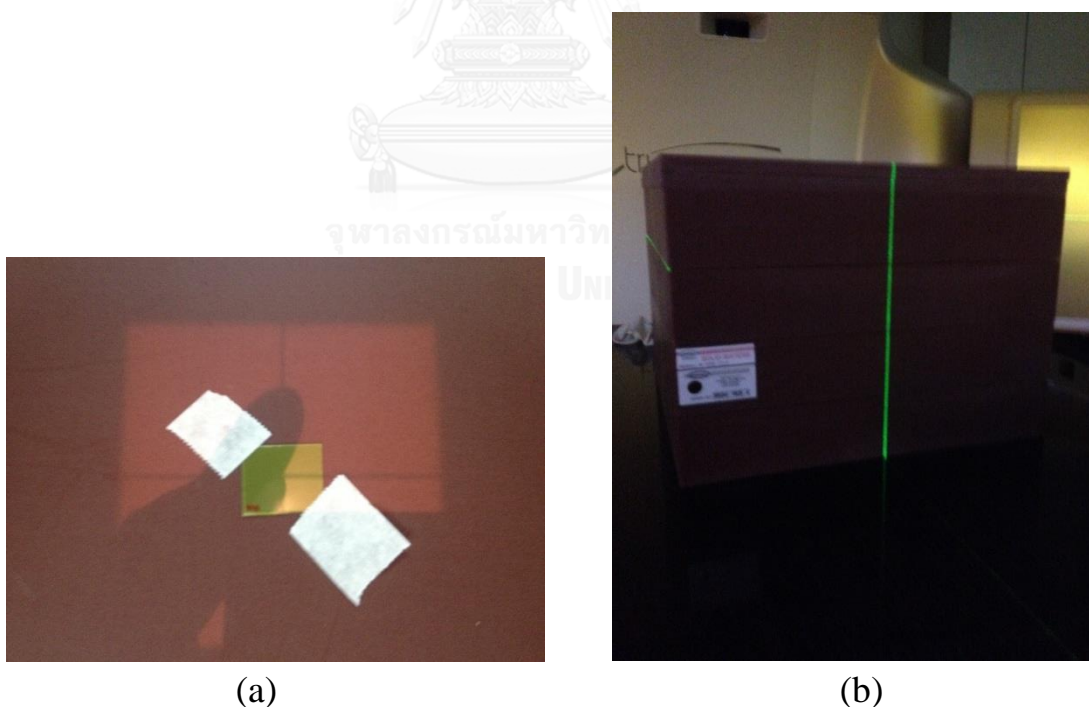


Figure 3.13 (a) The 2×2 cm² EBT3 film and (b) film calibration setting up in virtual slab phantom.

3.7.2 ArcCHECK calibration

The diode array (ArcCHECK) detector was set to 100 cm. SAD (86.7 cm SSD.), 0 degree gantry angle and 10×10 cm² field size. The detector was irradiated with 6 MV FFF photon beams and dose calibration was performed for 200 cGy, as shown in figure 3.14.

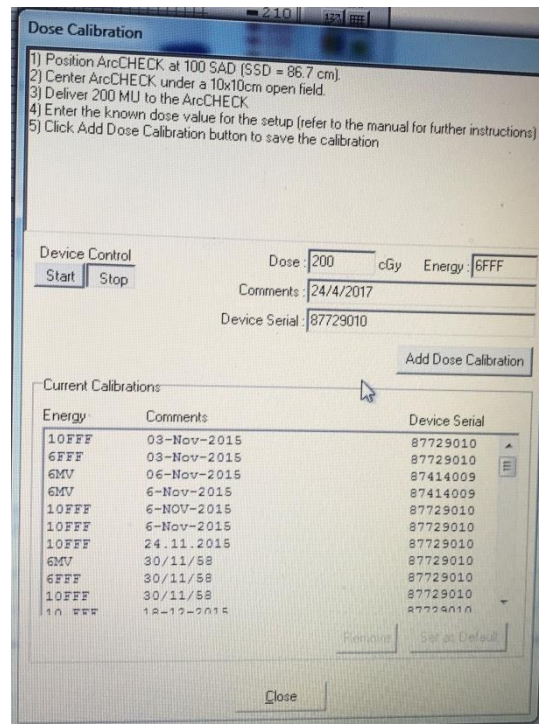


Figure 3.14 The dose calibration of detector diode array (ArcCHECK).

3.7.3 Point dose verification

For absolute dose measurement, there were two dosimetric systems. The first system was IBA CC13 ion chamber in ArcCHECK. The second system was IBA CC01 and CC13 ion chamber in Lucy phantom.

There were four steps.

3.7.3.1 VMAT verification plans

All ion chambers in both ArcCHECK and Lucy phantoms were scanned with CT-simulator to create CT images. After that, the lung VMAT SBRT plans of each patient were transferred to ArcCHECK phantom with CC13 chamber and in Lucy phantom with CC13 and CC01 chamber, they are shown in figure 3.15, 3.16 and 3.17, respectively. The planned doses were recalculated by Acuros XB algorithm and were compared to the measured dose.

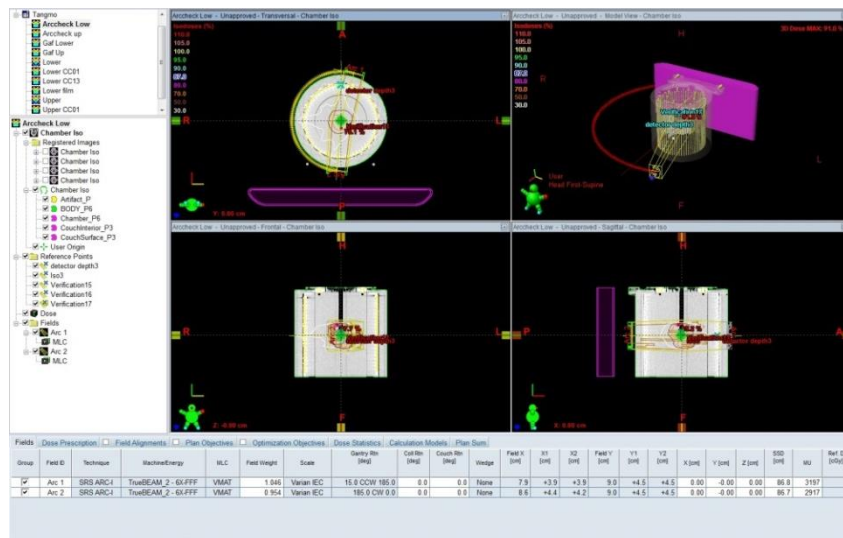


Figure 3.15 The VMAT QA plans for CC13 in ArcCHECK phantom.

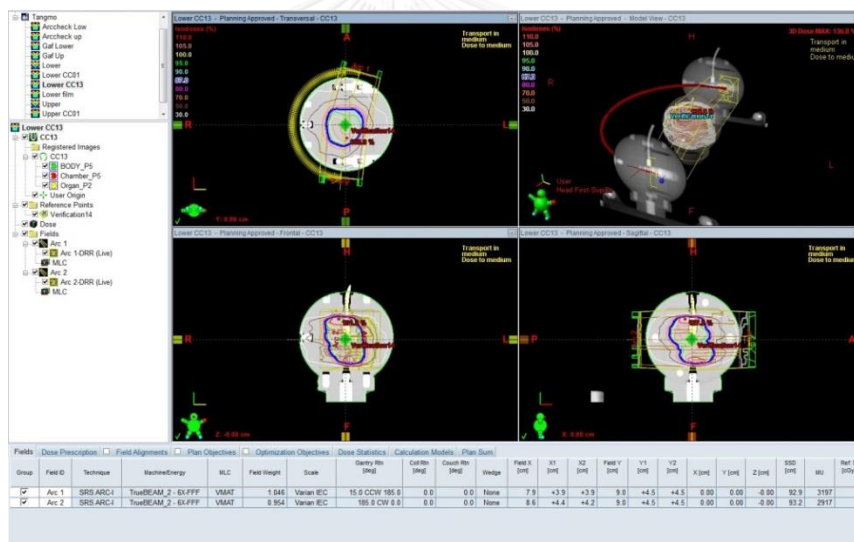


Figure 3.16 The VMAT QA plans for CC13 in Lucy phantom.

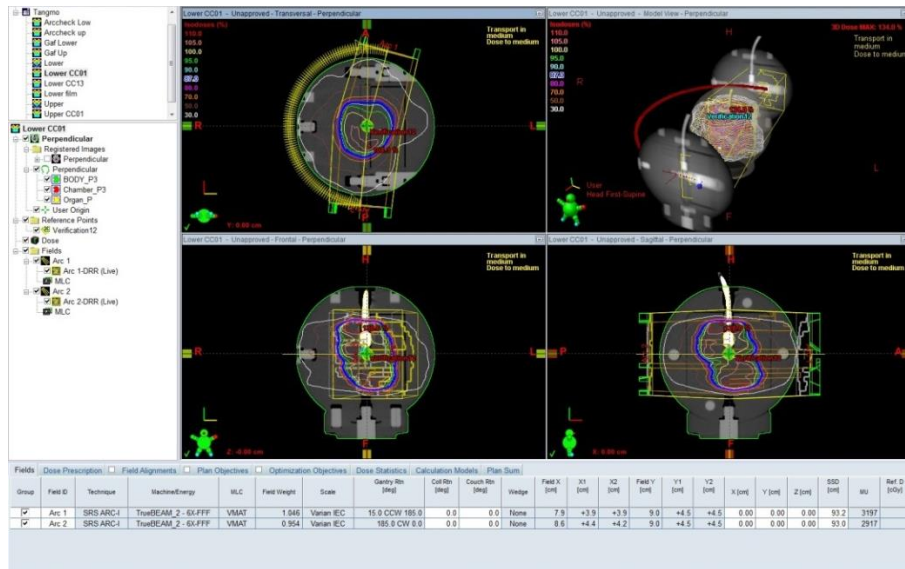


Figure 3.17 The VMAT QA plans for CC01 in Lucy phantom.

3.7.3.2 Plan export

All verification plans were exported from Varian Eclipse treatment planning system (version 11.0.31) to Varian TrueBeamTM machine for measurement.

3.7.3.3 Dosimeter and phantom set up

The CC13 ion chamber was inserted in the center of ArcCHECK phantom and Lucy phantom as shown in figure 3.18 and 3.19, respectively. The CC01 ion chamber was inserted in Lucy phantom as shown in figure 3.20.

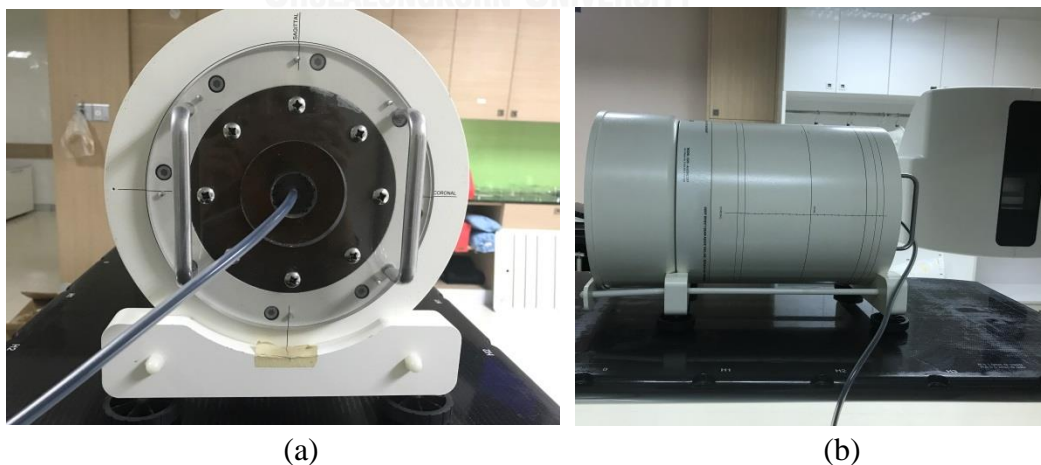


Figure 3.18 (a) The CC13 ion chamber inserted in ArcCHECK front view and (b) side view.



Figure 3.19 The CC13 ion chamber inserted in Lucy phantom.



Figure 3.20 The CC01 ion chamber inserted in Lucy phantom.

3.7.3.4 Measurement

The charges were counted by Dose-1 electrometer with +300 polarizing voltages and the charges were converted to dose, it is shown in figure 3.21.



Figure 3.21 The Dose-1 electrometer with +300 volt.

3.7.4 Dose distribution verification

For relative dose measurement, there were two dosimetric systems. The first system was diode array detector in ArcCHECK phantom. The second system was Gafchromic EBT3 film in Lucy phantom.

There were four steps for the verification.

3.7.4.1 VMAT verification plans

The film cassette in Lucy phantom and the diode array detector in phantom were scanned with CT-Simulator. After that, the lung VMAT SBRT plans for each patient were transferred to the ArcCHECK and Lucy phantom, they are shown in figure 3.22 and 3.23, respectively.

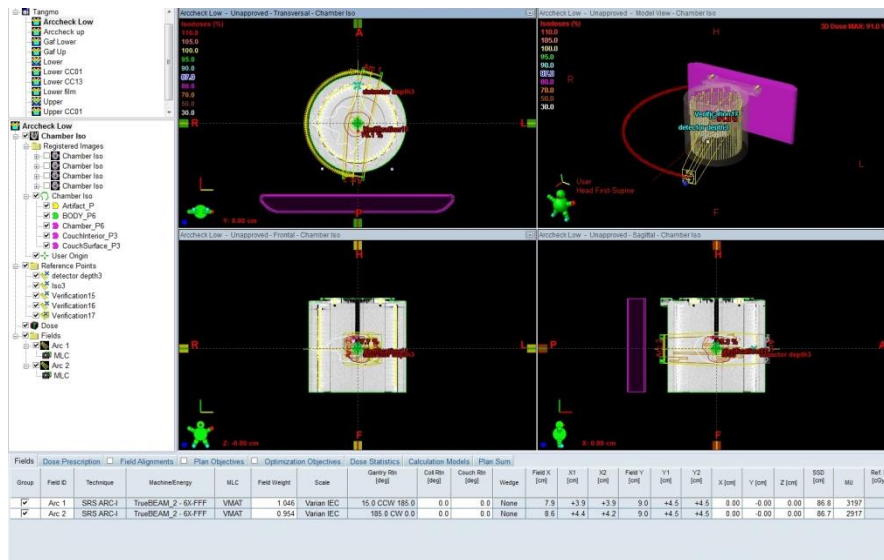


Figure 3.22 The VMAT QA plans for ArcCHECK phantom.



Figure 3.23 The VMAT QA plans for EBT3 film in Lucy phantom.

3.7.4.2 Plan export

All verification plans were exported from Varian Eclipse treatment planning system (version 11.0.31) to Varian TrueBeam machine for measurement.

3.7.4.3 Dosimeter and phantom setting

The EBT3 films were cut into $7.5 \times 7.5 \text{ cm}^2$ and were inserted in cassette. Then the cassette was inserted in Lucy phantom, it is shown in figure 3.24.

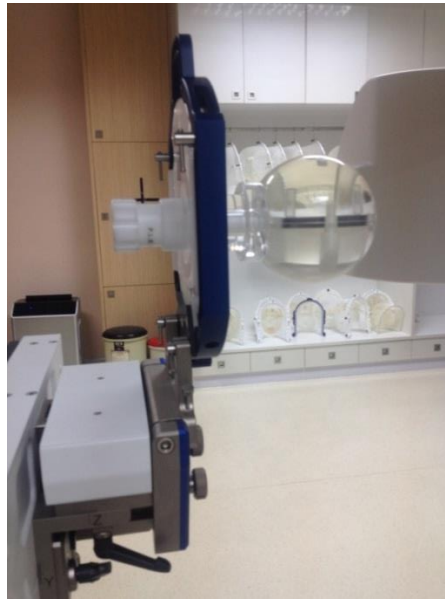


Figure 3.24 The EBT3 film inserted in Lucy phantom.

3.7.4.4 Film reading

After measuring, the EBT3 films, which were irradiated with 6 MV FFF beam, were left in room temperature overnight for stability for the color change. After that, the films were read by Epson film scanner, which is shown in figure 3.25.

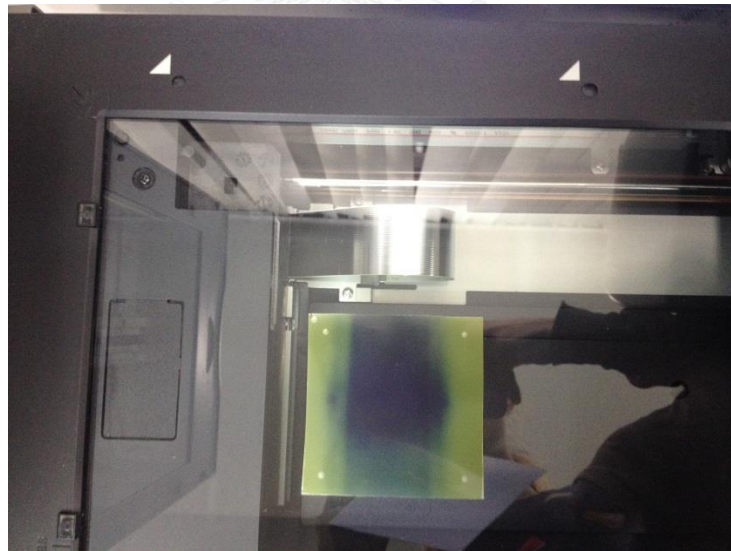


Figure 3.25 The EBT3 film reading by Epson film scanner.

3.7.5 Data collection

3.7.5.1 Point dose verification

The data were collected with ion chamber through Dose-1 electrometer in electric charges (nC). Then, the electric charges were converted to absorbed dose (cGy) according to equation 3.1 following IAEA TRS No. 398 [24].

$$D \text{ (cGy)} = M \times N_{D,w,Q_0} \times K_{TP} \times K_{Q,Q_0} \dots\dots\dots(3.1)$$

where D = Absorbed dose in water (cGy)
M = Reading of a dosimeter (nC)
 N_{D,w,Q_0} = Absorbed dose calibration factor (mGy/nC)
 K_{Q,Q_0} = Correction factor for beam quality
 K_{TP} = Correction factor for temperature pressure to the standard condition of calibration laboratory.

$$K_{TP} = \frac{(273.2+T) P_0}{(273+T_0) P} \dots\dots\dots(3.2)$$

3.7.5.2 Dose distribution verification

The data were collected in percent gamma pass between measured dose and calculated dose by SNC patient software.

3.7.6 Data analysis

3.7.6.1 Point dose verification

After measuring, the calculated dose and measured dose were compared by the percent point dose difference that calculated by equation 3.3. The percent point dose difference tolerance is within $\pm 3\%$ (control limit) and $\pm 5\%$ (action limit) [15].

$$\% \text{ Point dose difference} = \frac{\text{Calculated dose} - \text{Measured dose}}{\text{Measured dose}} \times 100\% \dots\dots\dots(3.3)$$

3.7.6.2 Dose distribution verification

After measuring, the calculated dose and measured dose were compared by Gamma pass index. The criteria used for comparison is the gamma

3.7.6.3 Statistical analysis

The percent point dose differences of measured dose and calculated dose of CC13 ion chamber in ArcCHECK, CC01 and CC13 ion chamber in Lucy phantom were compared with a paired t-test. The differences were considered in statistically significance for p-values < 0.05. A different sample t-test was also used to compare between the gamma pass of measuring with ArcCHECK and Gafchromic EBT3 film

3.8 Outcome measurement


Variable: Independent variables = Energy
 : Dependent variables = Size of ionization chamber, type of phantom, resolution of detector, response of detector

3.9 Benefit of the study

The suitable patient specific QA tools will be selected for lung SBRT.

3.10 Ethical consideration

Although this study was performed in phantom, however the ethical approval was processed by Ethics Committee of Faculty of medicine, Chulalongkorn University (IRB No. 513/59). The certificate is shown in figure 3.28.



INSTITUTIONAL REVIEW BOARD
Faculty of Medicine, Chulalongkorn University
 1873 Rama IV Road, Patumwan, Bangkok 10330, Thailand, Tel. 662-256-4493

COE No. 023/2016
 IRB No. 513/59

Certificate of Exemption

The Institutional Review Board of the Faculty of Medicine, Chulalongkorn University, Bangkok, Thailand, has exempted the following study in compliance with the International guidelines for human research protection as Declaration of Helsinki, The Belmont Report, CIOMS Guideline, International Conference on Harmonization in Good Clinical Practice (ICH-GCP) and 45CFR 46.101(b)

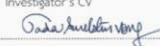

Study Title : Dosimetric comparison of patient specific QA in lung SBRT using unflattened beams between two dosimeter systems

Principal Investigator : Miss Sitanan Maknitikul

Study Center : Department of Radiology, Faculty of Medicine, Chulalongkorn University.

Document Approval :

1. Protocol Version 1.0 Date August 21, 2016
2. Protocol synopsis Version 1.0 Date August 11, 2016
3. Case record form Version 1.0 Date August 11, 2016
4. Investigator's CV

Signature:  **Signature:** 

(Emeritus Professor Tada Sueblinvong MD)
 Chairperson
 The Institutional Review Board

(Assistant Professor Prapapan Rajatapakdi MD, PhD)
 Member and Secretary
 The Institutional Review

Date of Exemption : September 13, 2016

Note No continuing review report and final report when finish require

Figure 3.28 The certificate of Approval from Ethic Committee of Faculty of Medicine Chulalongkorn University.

CHAPTER IV

RESULTS

4.1 Film calibration

The data of absorbed dose, pixel value and optical density of film calibration is shown in table 4.1. The relation between absorbed dose and pixel value (scanner response) was plotted and displayed in figure 4.1. The exponential curve was observed. The pixel value was decreased when the absorbed dose increased. The high gradient was illustrated in low dose region from 0 to 1,000 cGy and the low gradient started from 1,000 to 4,000 cGy.

Table 4.1 The data of dose, pixel value and optical density of film calibration.

Absorbed dose(cGy)	Pixel value (Red channel)	OD(Red channel)
0	40467.84	0.00
200	27504.24	0.18
400	21195.50	0.25
800	15497.76	0.30
1000	13947.54	0.31
1500	11479.00	0.33
2000	10121.17	0.34
2500	9212.83	0.35
3000	8444.93	0.36
4000	7700.31	0.36

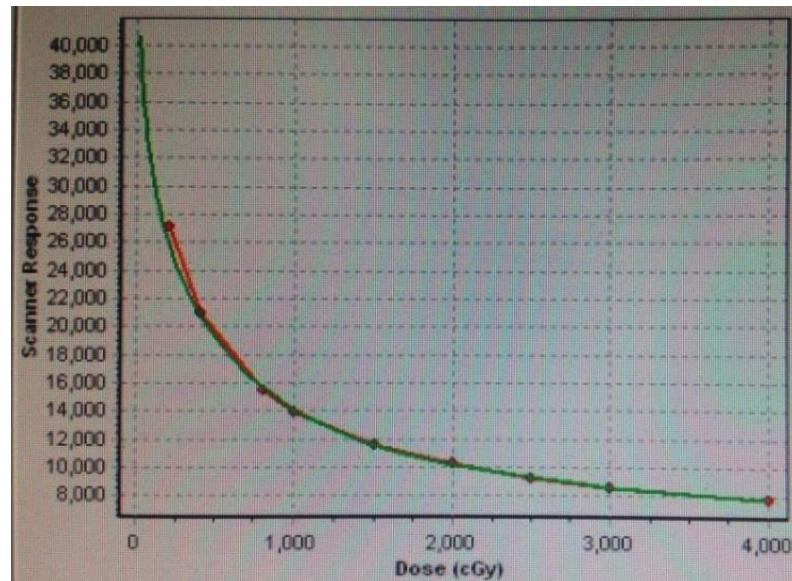


Figure 4.1 The film calibration curve between absorbed dose and pixel value.

4.2 Point dose verification

The details of treatment data for all patients and the measured values in both dosimetry systems are shown in appendix.

The measured doses from CC13 chamber in ArcCHECK phantom ranged from 324.1 to 2101.3 cGy for fifteen plans. The measured point dose, calculated point dose and point dose difference using CC13 ion chamber in ArcCHECK are shown in table 4.2.

Table 4.2 The measured, calculated point dose and point dose difference of fifteen plans using CC13 ion chamber in ArcCHECK.

Plan No.	Measured dose (cGy)	Calculated dose (cGy)	Point dose difference (%)
1	1433.0	1442.5	0.7
2	2101.3	2085.3	-0.8
3	838.1	820.9	-2.1
4	793.3	783.5	-1.2
5	750.5	745.1	-0.7
6	571.3	562.3	-1.6
7	720.9	666.0	-7.6
8	1032.9	1016.4	-1.6
9	324.1	320.3	-1.2
10	656.1	654.7	-0.2
11	831.5	845.8	1.7
12	1055.8	1019.7	-3.4
13	350.9	342.6	-2.4
14	1700.8	1701.7	0.1
15	1009.0	1024.9	1.6

The percent point dose difference of fifteen plans using CC13 ion chamber in ArcCHECK is presented in figure 4.2. The mean percent point dose difference, which is shown in table 4.7, is $-1.3 \pm 2.3\%$ with the range of -7.6 to 1.7%. The control limit is set at $\pm 3\%$ and action limit is set at $\pm 5\%$.

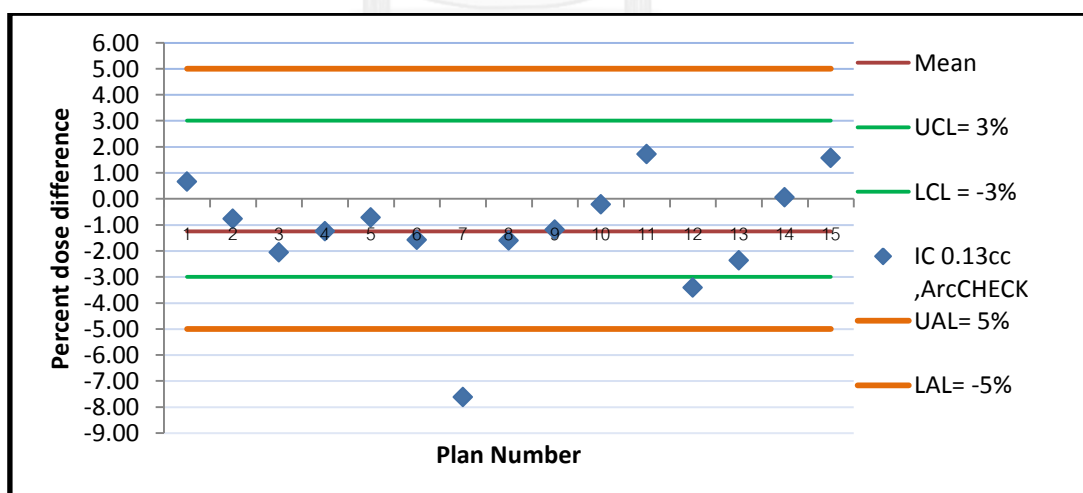


Figure 4.2 The scatter plot of percent point dose difference of fifteen plans using CC13 ion chamber in ArcCHECK.

The measured point dose, calculated point dose and point dose difference using CC13 and CC01 in Lucy phantom are shown in table 4.3 and 4.4, respectively.

Table 4.3 The measured, calculated point dose and point dose difference of fifteen plans using CC13 ion chamber in Lucy phantom.

Plan No.	Measured dose(cGy)	Calculated dose (cGy)	Point dose difference (%)
1	2135.3	2079.3	-2.6
2	2979.4	2949.1	-1.0
3	1186.3	1148.6	-3.2
4	1167.3	1180.0	1.1
5	1091.5	1109.3	1.6
6	803.8	768.3	-4.4
7	718.4	717.0	-0.2
8	1513.9	1583.8	4.6
9	456.0	439.7	-3.6
10	957.0	950.7	-0.7
11	1163.3	1147.0	-1.4
12	1491.8	1490.1	-0.1
13	482.1	481.7	-0.1
14	2441.1	2457.1	0.7
15	1464.6	1451.3	-0.9

Table 4.4 The measured, calculated point dose and point dose difference of fifteen plans using CC01 ion chamber in Lucy phantom.

Plan No.	Measured dose (cGy)	Calculated dose (cGy)	Point dose difference (%)
1	2087.5	2051.7	-1.7
2	2899.9	2897.5	-0.1
3	1145.2	1132.8	-1.1
4	1102.8	1109.3	0.6
5	1061.6	1043.5	-1.7
6	791.1	806.5	1.9
7	689.3	674.2	-2.2
8	1449.4	1395.3	-3.7
9	440.2	444.3	0.9
10	918.5	914.7	-0.4
11	1124.4	1100.4	-2.1
12	1454.8	1412.5	-2.9
13	468.2	464.3	-0.8
14	2416.9	2331.6	-3.5
15	1444.0	1390.5	-3.7

The percent point dose of fifteen plans using CC13 and CC01 ion chamber in Lucy phantom is shown in figure 4.3. The mean percent point dose with CC13 and

CC01 ion chamber, which are shown in table 4.7, were $-0.7 \pm 2.3\%$ with the range of -4.1 to 4.6% and $-1.4 \pm 1.8\%$ with the range of -3.7 to 1.9 %, respectively.

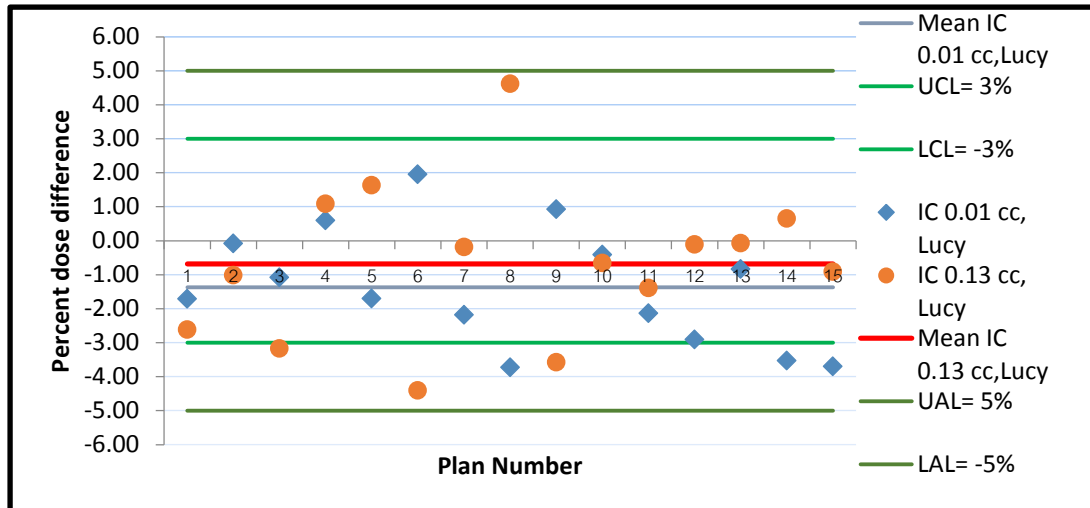


Figure 4.3 The scatter plot of percent point dose difference of fifteen plans using CC01 and CC13 ion chamber in Lucy phantom.

When the doses were compared in the same CC13 chamber but difference phantoms, we observed that the point dose differences from CC13 in ArcCHECK and Lucy phantom were mostly less than 3% difference. The 5 from 15 plans showed more than 3% difference as shown in table 4.5

Table 4.5 The difference between percent point dose of fifteen plans using CC13 ion chamber in ArcCHECK and Lucy phantom.

Plan no.	% point dose difference of CC13 in ArcCHECK	% point dose difference of CC13 in Lucy phantom	Dose difference (%)
1	0.7	-2.6	3.3
2	-0.8	-1.0	0.3
3	-2.1	-3.2	1.1
4	-1.2	1.1	-2.3
5	-0.7	1.6	-2.3
6	-1.6	-4.4	2.8
7	-7.6	-0.2	-7.4
8	-1.6	4.6	-6.2
9	-1.2	-3.6	2.4
10	-0.2	-0.7	0.5
11	1.7	-1.4	3.1
12	-3.4	-0.1	-3.3
13	-2.4	-0.1	-2.3
14	0.1	0.7	-0.6
15	1.6	-0.9	2.5

In case of the difference chambers in the same phantom, the point dose differences from two detectors were mostly less than 3% difference. The 5 plans showed more than 3% difference, the result is shown in table 4.6.

Table 4.6 The difference between percent point dose of fifteen plans using CC13 and CC01 ion chamber in Lucy phantom.

Plan No.	% point dose difference of CC13 in Lucy phantom	% point dose difference of CC01 in Lucy phantom	Dose difference (%)
1	-2.6	-1.7	0.9
2	-1.0	-0.1	0.9
3	-3.2	-1.1	2.1
4	1.1	0.6	-0.5
5	1.6	-1.7	-3.3
6	-4.4	1.9	6.4
7	-0.2	-2.2	-2.0
8	4.6	-3.7	-8.4
9	-3.6	0.9	4.5
10	-0.7	-0.4	0.2
11	-1.4	-2.1	-0.7
12	-0.1	-2.9	-2.8
13	-0.1	-0.8	-0.8
14	0.7	-3.5	-4.2
15	-0.9	-3.7	-2.8

The mean and range of percent point dose difference of one chamber in ArcCHECK and two different chambers in Lucy phantom including statistically significant differences of point dose difference between two dosimeter systems are shown in table 4.7. There were not statistically significant differences.

Table 4.7 The mean and range of percent point dose differences between measured dose and calculated dose and statistically significant differences of point dose difference between two systems. Differences are considered statistically significant for p-values < 0.05.

	% point dose differences			P-values	
	ArcCHECK CC13	Lucy CC13	Lucy CC01	CC13,ArcCH ECK vs CC13,Lucy	CC01,Lucy vs CC13,Lucy
Mean	-1.3±2.3	-0.7±2.3	-1.4±1.8	0.5	0.4
Range	-7.6 to 1.7	-4.4 to 4.6	-3.7 to 1.9		

4.3 Dose distribution verification

The percent gamma pass of fifteen plans using diode array detector in ArcCHECK and EBT3 film in Lucy phantom is shown in table 4.8.

Table 4.8 The percent gamma pass of fifteen plans using diode array detector in ArcCHECK and EBT3 film in Lucy phantom.

Plan No.	Gamma pass (%)	
	ArcCHECK	EBT3 film
1	93.7	94.7
2	94.8	91.9
3	96.6	91.2
4	95.3	89.6
5	96.4	90.0
6	93.8	94.3
7	98.4	84.8
8	95.6	99.1
9	97.7	80.7
10	95.4	98.3
11	93.8	97.7
12	92.3	96.1
13	91.7	83.9
14	94.3	99.1
15	93.5	97.5

The percent gamma pass of fifteen plans using diode array detector in ArcCHECK is presented in figure 4.4. The mean percent gamma pass, which is shown in table 4.9, was 94.9 ± 1.9 % with the range from 91.4 to 98.4%.

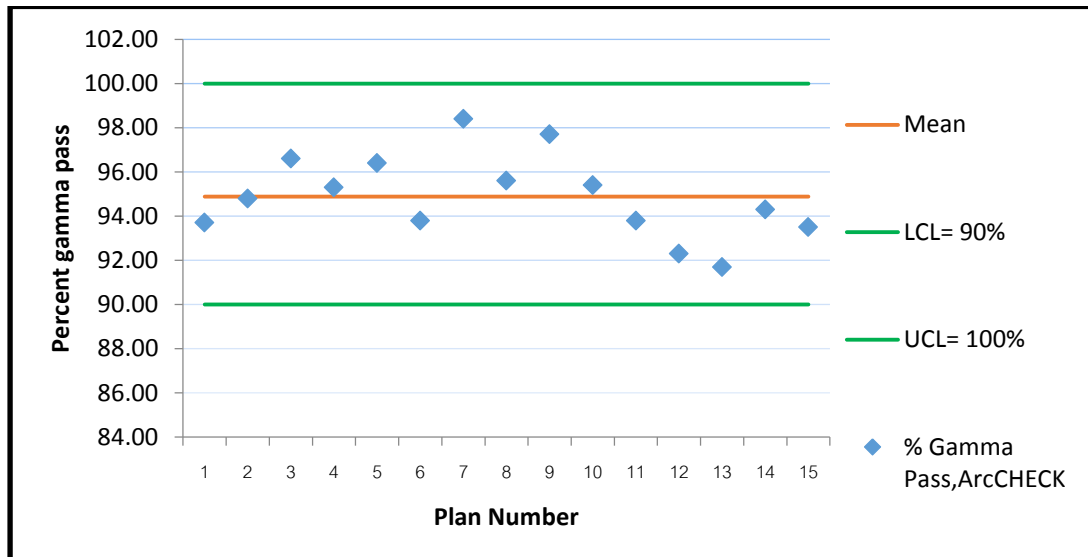


Figure 4.4 The scatter plot of percent gamma pass of fifteen plans using diode array detector in ArcCHECK.

The percent gamma pass of fifteen plans using EBT3 film in Lucy phantom is shown in figure 4.5. The mean percent gamma pass, which is shown in table 4.9, was 92.6 ± 5.9 % with the range from 80.7 to 99.1 %.

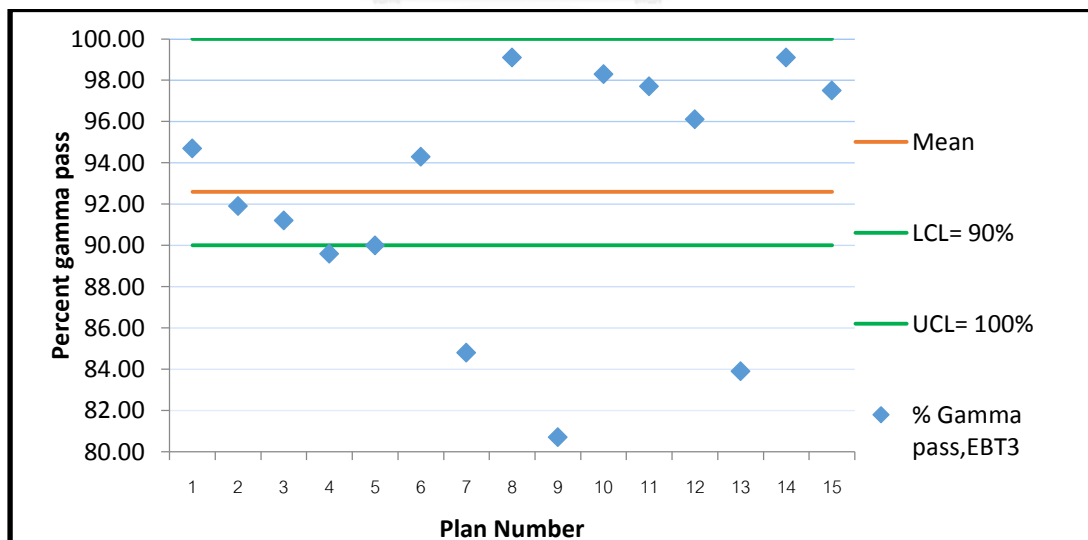


Figure 4.5 The scatter plot of percent gamma pass of fifteen plans using EBT3 film in Lucy phantom.

The mean and range of percent gamma pass of diode array detector in ArcCHECK and EBT3 in Lucy phantom including statistically significant differences of gamma pass between two dosimeter systems are shown in table 4.9. There were not statistically significant differences.

Table 4.9 The mean and range of percent gamma pass between measured dose and calculated dose and statistically significant differences of gamma pass between two systems. Differences are considered statistically significant for p-values < 0.05.

	% gamma pass		P-values
	ArcCHECK	EBT3 film in Lucy phantom	ArcCHECK vs EBT3 film
Mean	94.9 ± 1.9	92.6 ± 5.9	0.2
Range	91.4 to 98.4	80.7 to 99.1	



CHAPTER V

DISCUSSION AND CONCLUSION

5.1 Discussion

5.1.1 Point dose verification

For measurement with CC13 ion chamber in ArcCHECK, 13 plans from total of 15 plans were in control limit (within $\pm 3\%$), 14 plans passed in action limit (within $\pm 5\%$). One plan of large point dose difference of 7.6% was observed, the error might be due to position of ion chamber in high dose gradient. Therefore the point dose difference between measured dose and absorbed dose was high.

For measurement with CC13 ion chamber in Lucy phantom, 11 plans were passed in control limit (within $\pm 3\%$), and all plans were passed in action limit (within $\pm 5\%$).

For measurement with CC01 ion chamber in Lucy phantom, 12 plans were passed in control limit (within $\pm 3\%$). And all plans (15 plans) were passed in action limit (within $\pm 5\%$).

The two chambers of CC01 and CC13 in the same phantom showed agreeable. The differences between two chambers for 10 plans were less than 3%, The 5 plans were higher than 3% difference.

The percent point dose difference between CC01 and CC13 in Lucy phantom was not significant difference with p-value = 0.4.

The same chamber of CC13 in different phantom illustrated less agreeable than difference chamber in the same phantom. The difference of the same chamber between two phantoms of 10 plans were less than 3%, the 5 plans were higher than to 3% difference.

The percent point dose difference between CC13 in ArcCHECK and CC13 in Lucy phantom was not significant difference with p-value = 0.5.

Table 5.1 is the comparison of the mean of point dose between this study and other study. The mean of percent point dose difference of CC13 with Lucy phantom in this study ($0.7 \pm 2.3\%$) was slightly lower than Parmider Basran et al study (0.9%) [21]. The mean of percent point dose difference of CC01 with Lucy phantom in this study ($1.37 \pm 1.74\%$) was higher than Ryan D. Foster et al. study (0.8%) [25] that might be due to the different phantom used. However, all of studies were passed within $\pm 3\%$ criteria.

Table 5.1 The comparison of percent point dose difference between this study, Ryan et al. and Parmider et al. studies.

	This study		Ryan D. Foster et al. [25]	Parmider Basran et al. [21]
Dosimetry System	CC13/ Lucy phantom	CC01/ Lucy phantom	PTW 31014 (0.01cc) / anthropomorphic thorax phantom	PTW 31010 (0.13 cc) / Lucy phantom
% dose difference measured and calculated	0.7±2.3	1.4±1.7	0.8	0.9

5.1.2 Dose distribution verification

For measurement with diode array detector in ArcCHECK, all plans (fifteen plans) were in good agreement with gamma passing rate above 90%.

For measurement with EBT3 film in Lucy phantom, 12 plans were passed in criteria (above 90%), and 3 plans: plans number 7, 9 and 13 which are shown in table 5.2, were not agreed.

The disagreement may attribute to the limitation of dose response in Gafchromic film, especially in low dose region. From the calibration curve, which is shown in figure 4.1, the film was not good response in low dose region because of the high gradient of the response curve (around 400 to 1000 cGy) and also high dose region due to the very low gradient of the response curve (around 3,000 to 4,000 cGy), see in table 5.2, therefore the range of good dose response of Gafchromic EBT3 films was needed to test before using.

However, the relative gamma pass between diode array detector in ArcCHECK and EBT3 film in Lucy phantom was not significant difference with p-value of 0.2. This result implied that both systems can be used for dose distribution verification in lung SBRT plans.

Table 5.2 The percent gamma pass, measured dose and calculated dose of fifteen plans using EBT3 film in Lucy phantom.

EBT3 in LUCY phantom			
Plan No.	% gamma pass	Measured dose (cGy)	Calculated dose (cGy)
1	94.7	2087.5	2051.7
2	91.9	2900.0	2897.5
3	91.2	1145.2	1132.8
4	89.6	1102.8	1109.3
5	90.0	1061.6	1043.5
6	94.3	791.1	806.5
7	84.8	689.3	674.2
8	99.1	1449.4	1395.3
9	80.7	440.2	444.3
10	98.3	918.5	914.7
11	97.7	1124.4	1100.4
12	96.1	1454.8	1412.5
13	83.9	468.2	464.3
14	99.1	2416.9	2331.6
15	97.5	1444.0	1390.5

Table 5.3 is the comparison of the mean of percent gamma pass using diode array detector in ArcCHECK between this study and other studies.

The mean of percent gamma pass of this study ($94.9\pm 1.9\%$) was lower than Christian et al. ($98.0\pm 1.7\%$) [20] and Vibha et al. (98.3%) [22] study. However, all of studies were passed criteria above 90%.

Table 5.3 The comparison of the mean of percent gamma pass using diode array detector in ArcCHECK between this study, Christian et al. and Vibbha et al. study.

	This study	Christian R. Hansen et al. [20]	Vibha Chaswal et al. [22]
Dosimeter system	diode array detector/ ArcCHECK	diode array detector/ ArcCHECK	diode array detector/ ArcCHECK
% gamma pass between measurement and calculation	94.9±1.9	98.0±1.7	98.3

Table 5.4 is the comparison of the mean of percent gamma pass using EBT3 film in different phantoms between this study and other study. The mean percent gamma pass of this study ($92.6\pm 5.9\%$) was lower than Davide Cusumano et al. (94.3%) [23] and Jin-Beom et al. study ($96.2\pm 2.5\%$) [26], it might be due to the large error in low dose cases selected. However, all of studies were pass criteria with the average gamma index value above 90%.

Table 5.4 The comparison of the mean of percent gamma pass using EBT3 film in different phantoms between this study Davide et al and Jin-Beom et al. study.

	This study	Davide Cusumano et al. [23]	Jin-Beom et al. [26]
Dosimeter system	EBT3/Lucy phantom	EBT3/ EasyCube cubic phantom	EBT3/cylindrical acryl phantom
% gamma pass measured and calculated dose	92.6±5.9	94.3	96.2±2.5

5.2 Conclusion

Patient specific QA is the procedure of verification to ensure that each individual patient's treatment plan conforms to deliver as planned. In advance technique, the patient specific QA tool is needed for more accuracy. This study was to determine the different patient specific QA tool between two volume sizes of 0.01 and 0.13 CC ion chamber for point dose and between diode array detector in ArcCHECK and Gafchromic film in Lucy phantom for dose distribution in VMAT lung SBRT using unflattened photon beams.

For point dose verification, the point dose difference between measured and calculated dose for almost all of the plans were within criteria of $\pm 3\%$.

The dose differences of two chambers (CC13 and CC01) in the Lucy phantom were mostly less than 3%. Therefore, the percent point dose difference between CC13 and CC01 in Lucy phantom was not significant difference.

The differences of the same chamber of CC13 in different phantom were also mostly less than 3%. Therefore, the percent point dose difference between CC13 in ArcCHECK and CC13 in Lucy phantom was not significant difference.

For dose distribution verification, the percent gamma pass between measured and calculated dose for most of plans were above 90%. The gamma pass between diode array detector in ArcCHECK and EBT3 film in Lucy phantom was not significant difference.

Therefore, the effect on volume of chamber and phantom were not statistical significant difference.

However, some dosimeters have limitation such as IBA CC13 ion chamber, the position of chamber affected to percent dose difference. The volume of the chamber may be in the high dose gradient area causing the average dose reading. For IBA CC01 ion chamber, all of plans passed within criteria, so the CC01 ion chamber can be used for lung VMAT SBRT plans. The diode array detectors in ArcCHECK phantom spaced 1 cm spacing between detectors, so the ArcCHECK could not be used for very small target volume due to these low resolution detectors. The Gafchromic EBT3 film is good responded in some dose region. The dose range in each plan must be careful considered before performing the measurement.

5.3 Recommendation

The range of dose response of Gafchromic EBT3 film maybe affected to measurement, therefore the dose response of the film is needed to test before using.

REFERENCES

1. Benedict, S.H., et al., *Stereotactic body radiation therapy: the report of AAPM Task Group 101*. Medical Physics, 2010. **37**(8): p. 4078-4101.
2. Khan, F.M., *The Physics of Radiation Therapy* Fifth ed. 2014, Philadelphia, PA 19103 USA: Lippincott Williams and Wilkins.
3. Schell, M.C., J.F. Bova, and D.V. Larson, *Stereotactic radiosurgery: the report of AAPM Task Group 42* Medical Physics, 1995.
4. Blomgren, H., I. Lax, and I. Naslund, *Stereotactic high dose fraction radiation therapy of extracranial tumors using an accelerator. Clinical experience of the first thirty-one patients*. Acta Oncologica, 1995. **34**: p. 861-870.
5. Benzil, D.L., et al., *Safety and efficacy of stereotactic radiosurgery for tumors of the spine*. Journal of Neurosurgery, 2004. **101**: p. 413-418.
6. Yu, C., *Intensity-modulated arc therapy with dynamic multi-leaf collimation: an alternative to tomotherapy*. Physics in Medicine and Biology, 1995. **40**: p. 1435-1449.
7. Mancuso, G.M., *Evaluation of volumetric modulated arc therapy (VMAT) patient specific quality assurance*, in *The Department of Physics and Astronomy*. 2011, The Louisiana State University.
8. Laojunun, P., *Evaluation of planar and cylindrical diode array for IMRT and VMAT plan verification*, in *The Faculty of Graduated*. 2014, Mahidol University: Bangkok, Thailand.
9. Rao, M., et al., *Comparison of Elekta VMAT with helical tomotherapy and fixed field IMRT: Plan quality, delivery efficiency and accuracy*. Medical Physics, 2010. **37**: p. 1350-1359.
10. Otto, K., M. Milete, and J. Wu, *Temporal delivery efficiency of a novel single gantry arc optimization technique for treatment of recurrent nasopharynx cancer*. International Journal of Radiation Oncology, 2007. **69**.
11. Otto, K., *Volumetric modulated arc therapy: IMRT in a single gantry arc*. Medical Physics, 2008. **35**: p. 310-317.
12. Plama, D., et al., *Volumetric modulated arc therapy for delivery of prostate radiotherapy: comparison with intensity-modulated radiotherapy and three-dimensional conformal radiotherapy*. International Journal of Radiation Oncology, 2008. **72**: p. 996-1001.

13. Ahlström, M., *Flattening filter free volumetric modulated arc therapy for extreme hypo-fractionation of prostate cancer decreasing the treatment time and reducing the impact of prostate motion*, in *Department of Medical Radiation Physics*. 2015, Lund University.
14. Ramsey, C.R., D. Dube, and W.R. Hendee, *It is necessary to validate each individual IMRT treatment plan before delivery*. *Medical Physics*, 2003. **30**(2271-2273).
15. Ezzell, G.A., et al., *IMRT commissioning: multiple institution planning and dosimetry comparisons, a report from AAPM Task Group 119*. *Med Phys*, 2009. **36**(11): p. 5359-5373.
16. Low, D.A., B.H. William, and M. Sasa, *A technique for the quantitative evaluation of dose distributions*. *Medical Physics*, 1998. **5**.
17. Van, D.J., et al., *Commissioning and quality assurance of treatment planning computers*. *International Journal of Radiation Oncology*, 1993. **26**: p. 261-273.
18. García-Garduño, O.A., et al., *Effect of dosimeter type for commissioning small photon beams on calculated dose distribution in stereotactic radiosurgery*. *Medical Physics*, 2014. **41**(9).
19. Niroomand, A., et al., *Radiochromic film dosimetry: Recommendations of AAPM Radiation Therapy Committee Task Group 55*. *Medical Physics*, 1998. **25**(11).
20. Hansen, C.R., et al., *Plan quality and delivery accuracy of flattening filter free beam for SBRT lung treatments*. *Acta Oncologica*, 2015. **54**(3): p. 422-427.
21. Basran, P. and C. Yeboah, *Dosimetric verification of micro-MLC based intensity modulated radiation therapy*. *Journal of applied clinical medical physics*, 2008. **9**(3): p. 109-121.
22. Chaswal, V., M. Weldon, and N. Gupta, *Commissioning and comprehensive evaluation of the ArcCHECK cylindrical diode array for VMAT pretreatment delivery QA*. *Journal of applied clinical medical physics*, 2014. **15**(4): p. 212-225.
23. Cusumano, D., et al., *Dosimetric verification of stereotactic radiosurgery/stereotactic radiotherapy dose distributions using Gafchromic EBT3*. *Medical Dosimetry*, 2015. **40**(3): p. 226-231.
24. IAEA, *Absorbed dose determination in external beam radiotherapy: Technical reports series No.398*. 2000, Vienna, Austria: INTERNATIONAL ATOMIC ENERGY AGENCY

25. Foster, R.D., M.P. Speiser, and T.D. Solberg, *Commissioning and verification of the collapsed cone convolution superposition algorithm for SBRT delivery using flattening filter-free beams*. Journal of applied clinical medical physics, 2013. **15**(2): p. 39-49.
26. Chung, J.B., et al., *Comparison of Dosimetric Performance among Commercial Quality Assurance Systems for Verifying Pretreatment Plans of Stereotactic Body Radiotherapy Using Flattening-Filter-Free Beams*. Journal Korean Medical Science, 2016. **31**(11): p. 1742-1748.



APPENDIX

Table A1. The treatment data of fifteen lung VMAT SBRT plans.

Plan No.	Technique	Tumor volume (cm ³)	Field size (cm ²)	No. of Arc	Prescribed dose (dose per Fr. (cGy))	No. of Fraction	Total dose (cGy)
1	VM SBRT lung	10.9	4x5	2	1500	3	4500
2	VM SBRT lung lower	145.3	8x9	2	2500	1	2500
3	VM SBRT lung upper	170.7	11x10	2	1000	3	3000
4	VM SBRT Rt.Lung	22.4	5x5	2	1000	5	5000
5	VM SBRT Lt. lung	7.5	6x5	2	1000	5	5000
6	VM SBRT lung	318.4	12x10	1	1000	3	3000
7	VM SBRT lung	8.8	4x4	2	1000	5	5000
8	VM SBRT lung	19.9	5x5	1	3000	1	3000
9	VM SBRT lung	25.8	18x14	3	400	5	2000
10	VM SBRT lung	65.5	8x8	2	700	8	5600
11	VM SBRT lung	73.8	7x7	2	1200	5	6000
12	VM SBRT lung	86.1	5x8	3	1200	5	6000
13	VM SBRT lung	266.5	14x14.5	3	500	10	5000
14	VM SBRT lung	18.6	4.6x4.8	2	1800	3	5400
15	VM SBRT lung	81.1	8x7	3	1200	5	6000

Table A2. The measured dose, calculated dose and percent point dose difference of fifteen lung VMAT SBRT plans using CC13 in ArcCHECK.

Plan No.	Measured (nC)	Measured dose (cGy)	Calculate dose (cGy)	Minimum of calculate dose (cGy)	Maximum of calculate dose (cGy)	Point dose difference (%)
1	54.4	1433.0	1442.5	1453.7	1545.6	0.7
2	77.5	2101.3	2085.3	1998.5	2075.2	-0.8
3	30.9	838.1	820.9	788.4	829.1	-2.0
4	29.2	793.3	783.5	722.6	761.7	-1.2
5	27.7	750.5	745.1	700.8	740.1	-0.7
6	21.2	571.3	562.3	531.0	595.2	-1.6
7	26.7	720.9	666.0	647.5	688.3	-7.6
8	38.2	1032.9	1016.4	883.0	1035.5	-1.6
9	12.0	324.1	320.3	303.1	320.9	-1.2
10	24.3	656.1	654.7	626.5	647.0	-0.2
11	30.6	831.5	845.8	789.5	856.9	1.7
12	38.8	1055.7	1019.7	958.4	1018.2	-3.4
13	12.9	350.9	342.6	331.7	344.7	-2.4
14	62.6	1700.8	1701.7	1537.1	1685.1	0.1
15	37.1	1009.0	1024.9	957.3	1025.5	1.6

Table A3. The measured dose, calculated dose and percent point dose difference of fifteen lung VMAT SBRT plans using CC01 in Lucy phantom.

Plan No.	Measured (nC)	Measured dose(cGy)	Calculated dose (cGy)	Minimum of calculated dose (cGy)	Maximum of calculated dose (cGy)	Pont dose difference (%)
1	6.7	2087.5	2051.7	2024.1	2091.3	-1.7
2	9.4	2900.0	2897.5	2876.7	2925.6	-0.1
3	3.7	1145.2	1132.8	1113.1	1156.6	-1.1
4	3.6	1102.8	1109.3	1095.8	1138.0	0.6
5	3.4	1061.6	1043.5	1027.7	1062.1	-1.7
6	2.6	791.1	806.5	785.3	832.1	1.9
7	2.2	689.3	674.2	656.9	696.3	-2.2
8	4.7	1449.4	1395.3	1332.0	1493.4	-3.7
9	1.4	440.2	444.3	439.5	450.7	0.9
10	3.0	918.5	914.7	906.5	924.4	-0.4
11	3.6	1124.4	1100.4	1085.5	1118.7	-2.1
12	4.7	1454.8	1412.5	1388.2	1436.7	-2.9
13	1.5	468.2	464.3	461.0	470.4	-0.8
14	7.8	2416.9	2331.6	2277.1	2403.7	-3.5
15	4.7	1444.0	1390.5	1368.4	1418.2	-3.7

Table A4. The measured dose, calculated dose and percent point dose difference of fifteen lung VMAT SBRT plans using CC13 in Lucy phantom.

Plan No.	Measured (nC)	Measured dose (cGy)	Calculated dose(cGy)	Minimum of calculated dose (cGy)	Maximum of calculated dose (cGy)	Point dose difference (%)
1	77.8	2135.3	2079.3	2023.8	2121.7	-2.6
2	108.5	2979.4	2949.1	2889.7	3003.7	-1.0
3	43.2	1186.3	1148.6	1116.8	1195.2	-3.2
4	42.5	1167.3	1180.0	1133.8	1263.8	1.1
5	39.8	1091.5	1109.3	1058.2	1166.4	1.6
6	29.3	803.8	768.3	710.0	821.7	-4.4
7	26.2	718.4	717.0	676.5	773.3	-0.2
8	55.1	1513.9	1583.8	1348.8	1673.2	4.6
9	16.6	456.0	439.7	425.0	452.4	-3.6
10	34.9	957.0	950.7	918.6	983.2	-0.7
11	42.4	1163.3	1147.0	1109.5	1200.2	-1.4
12	54.4	1491.8	1490.1	1446.7	1525.9	-0.1
13	17.6	482.1	481.7	472.0	492.5	-0.1
14	89.0	2441.1	2457.1	2363.2	2508.2	0.7
15	53.4	1464.6	1451.3	1413.0	1474.4	-0.9

Table A5. The percent gamma pass of fifteen lung VMAT SBRT plans using diode array in ArcCHECK.

Plan No.	Gamma Pass (%)
	Absolute (%)
1	93.7
2	94.8
3	96.6
4	95.3
5	96.4
6	93.8
7	98.4
8	95.6
9	97.7
10	95.4
11	93.8
12	92.3
13	91.7
14	94.3
15	93.5

Table A6. The percent gamma pass of fifteen lung VMAT plans using EBT3 films in Lucy phantom.

Plan No.	Gamma pass (%)
	Relative (%)
1	94.7
2	91.9
3	91.2
4	89.6
5	90.0
6	94.3
7	84.8
8	99.1
9	80.7
10	98.3
11	97.7
12	96.1
13	83.9
14	99.1
15	97.5

VITA

Name: Miss Sitanan Maknitikul

Date of Birth: 29 December 1992

Place of Birth: Samut Prakan

Institutions Attended: Mahidol University, 2014

Bachelor of Science (Radiological Technology)

B.Sc. (Radiological Technology)

Home Address: 1856/140 Thepharak Road, Thepharak sub-district,
Mueang Samut Prakan District, Samut Prakan,
Thailand. 10270